PM
84
9,II

DOT/FAA/PM-84/9,II

Program Engineering
and Maintenance Service
Washington, D.C. 20591

FAA WJH Technical Center
00093439

GENERAL AVIATION ADMINISTRATION

JUL 21 1986

TECHNICAL CENTER LIBRARY
ATLANTIC CITY, N.J. 08405

Mechanistic Methodology for Airport Pavement Design with Engineering Fabrics

Vol. II: Advanced Concepts, Validation, and Criteria

Kamran Majidzadeh
George Ilves
V.R. Kumar

Resource International, Inc.
281 Enterprise Drive
Columbus, Ohio 43081

May 7, 1986
Final Report

This Document is available to the public through the National Technical Information Service, Springfield, Virginia 22161.

FAA WJH Technical Center
Tech Center Library
Atlantic City, NJ 08405

AVAILABLE IN
ELECTRONIC FORMAT

U.S. Department of Transportation
Federal Aviation Administration

NOTICE

This document is disseminated under the sponsorship of the Department of Transportation in the interest of information exchange. The United States Government assumes no liability for its contents or use thereof.

Technical Report Documentation Page

1. Report No.	2. Government Accession No.	3. Recipient's Catalog No.
DOT/FAA/PM-84/9, II		

4. Title and Subtitle	5. Report Date
Mechanistic Methodology for Airport Pavement Design with Engineering Fabrics, Volume II Advanced Concepts, Validation, and Criteria	May 7, 1986
	6. Performing Organization Code
	8. Performing Organization Report No.
7. Author(s) Kamran Majidzadeh, George J. Ilves, V.R. Kumar	
9. Performing Organization Name and Address Resource International, Inc. 281 Enterprise Drive Columbus, Ohio 43081	10. Work Unit No. (TRAIS)
	11. Contract or Grant No. DTFA01-81-C-10043
12. Sponsoring Agency Name and Address U.S. Department of Transportation Federal Aviation Administration 800 Independence Avenue, SW Washington, D.C. 20591	13. Type of Report and Period Covered Final
	14. Sponsoring Agency Code

15. Supplementary Notes

FAA Project Manager : Dr. Aston McLaughlin

16. Abstract

This report is Volume II of a two volume set dealing with the application of non-woven fabrics to rigid airport pavements to control and/or retard the development of reflection cracking of flexible overlays due to both thermal stresses and load-associated fatigue. This volume describes the development of a new viscoelastic analysis model for the analysis of thermal cracking that utilizes fundamental material properties and does not rely on phenomenological distress functions. The methods developed in this work as well as those presented in Phase I (Volume I), have been validated on one airport and four highway projects. The validation is described in this report and shows that the developed analysis models predict the reflection cracking phenomenon for all projects very well.

This report also describes the laboratory evaluation of a fiber-asphalt SAMI layer that shows promise for use in reflection cracking control. Finally, specifications for material properties, testing procedures, and construction methods are presented.

17. Key Words	18. Distribution Statement
Engineering Fabrics, Reflection Cracking, Overlay Design, Fatigue Cracking, Viscoelastic Analysis, Thermal Stresses, Joint Movement	No Restrictions. This document is available to the public through the National Technical Information Services, Springfiled, Virginia 22161

19. Security Classif. (of this report)	20. Security Classif. (of this page)	21. No. of Pages	22. Price
Unclassified	Unclassified	93	

Form DOT F 1700.7 (8-72) Reproduction of completed page authorized

PREFACE

This report reflects the part of the mission of the Federal Aviation Administration (FAA) to provide guidelines to airport owners and operators for cost effective rehabilitation techniques for airport pavements.

This research project entitled "Mechanistic Methodology For Airport Pavement Design With Engineering Fabrics", DTFA01-81-C-10043, was conducted by Resource International Inc., Westerville, Ohio. The project was sponsored by the Federal Aviation Administration (FAA).

During the preparation of this report, Dr. Aston McLaughlin was Technical Monitor for the Federal Aviation Administration.

TABLE OF CONTENTS

		Page
Preface		i
List of Figures		iv
List of Tables		v
CHAPTER I.		
INTRODUCTION		1
CHAPTER II.		
LABORATORY TESTING		
2.1	Types of Testing	3
2.2	Fabric Selection	5
2.3	Mix Design	6
2.3.1	Portland Cement Concrete Beams	6
2.3.2	Asphalt Concrete	8
2.4	Sample Preparation	10
2.5	Laboratory Testing	12
2.5.1	Fatigue Testing	12
2.5.2	Horizontal and Vertical Stresses	14
CHAPTER III.		
DATA ANALYSIS, METHODS AND MODELS		
3.1	Fatigue Life	17
3.2	Development of a Mechanistic Model for Thermal Stress Analysis	26
3.2.1	Crack Initiation and Propagation in Viscoelastic Media	27
3.2.2	Boundary Value Problem Solution	29
3.2.3	Determination of the Cohesive Zone Size, α	31
3.2.4	Determining the Viscoelastic Displacement, Uve	31
3.2.5	Determination of the Failure Time	32
3.2.6	Effect of Fabric on the Crack Opening Displacement and Failure Time Prediction	36
3.2.7	Analysis of Field Pavements	37
3.3	Laboratory Thermal Stress Tests	38
3.4	Application to Pavements	43
CHAPTER IV		
FIELD EVALUATION		
4.1	Introduction	46
4.2	Site Selection	46
4.3	Field Evaluation	47
4.4	Field Validation	47
4.4.1	Overlays Without Fabric Reinforcement	51

4.4.2 Overlays with Fabric Reinforcement 56
4.4.3 Summary of Field Evaluation 59

CHAPTER V

SPECIFICATIONS FOR MATERIAL PROPERTIES, TESTING PROCEDURES, AND CONSTRUCTION METHODS

5.1 Introduction 60
5.2 Materials 61
5.2.1 Physical Properties 62
5.2.2 Packaging Requirements 62
5.2.3 Identification Requirements 62
5.2.4 Sampling Requirements 62
5.2.5 Acceptance Criteria 62
5.2.6 Testing Requirements 64
5.3 Construction Methods 66

CHAPTER VI

CONCLUSIONS AND RECOMMENDATIONS

6.1 Conclusions 70
6.1.1 RECK Model 70
6.1.2 Use of Fabrics for Cracking Retardation 71
6.2 Recommendations on the Use of Fabrics 72
6.3 Recommendations for Future Research 73

REFERENCES 75

APPENDIX A 77

THE RECK PROGRAM

APPENDIX B 81

Theoretical analysis of small scale beams described in Mechanistic Methodology for Airport Pavement Design with Engineering Fabrics, Volume I: Theoretical and Experimental Bases.

LIST OF FIGURES

		Page
Figure 1.	Fatigue Test Set-Up	4
Figure 2.	Gradation of Concrete Aggregate	9
Figure 3.	Gradation of P-401 Asphalt Concrete Mix	9
Figure 4.	Marshall mix design data for P-401	11
Figure 5.	Laboratory Simulation of Overlaid Concrete Pavement	13
Figure 6.	Test set-up for simulated thermal loads	15
Figure 7.	Laboratory fatigue data for fiber sami at 40 and 72 °F	20
Figure 8.	Comparison of fatigue lives at 40 F (4°C)	21
Figure 9.	Comparison of fatigue lives at 72 F (22°C)	22
Figure 10.	Comparison of fatigue lives at 40 F (4°C)	23
Figure 11.	Comparison of fatigue lives at 72 F (21°C)	24
Figure 12.	Crack in a Viscoelastic Medium	28
Figure 13.	Results of Horizontal Pull Tests	39
Figure 14.	Comparison of Actual and Predicted Joint Opening for Small-Scale Beams	44
Figure 15.	Data Collection Plan	48
Figure 16.	Joint opening vs time for small-scale beams	82
Figure 17.	Joint opening vs time for small-scale beams	83
Figure 18.	Joint opening vs time for small-scale beams	84
Figure 19.	Joint opening vs time for small-scale beams	85
Figure 20.	Joint opening vs time for small-scale beams	86
Figure 21.	Joint opening vs time for small-scale beams	87

LIST OF TABLES

		Page
Table 1.	Polymer concrete mix data	7
Table 2.	Gradation limits of aggregate	7
Table 3.	Gradation of P-401 asphalt concrete	10
Table 4.	Fatigue Parameters	19
Table 5.	Results of horizontal pull tests	42
Table 6.	Coefficient of friction for various materials	45
Table 7.	Project data for unreinforced overlays	51
Table 8.	Analysis for project 5S	53
Table 9.	Analysis for project 9L	53
Table 10.	EFRON analysis for project 29	54
Table 11.	EFRON analysis for project 29a	54
Table 12.	Predicted failure times	56
Table 13.	Project data for fabric reinforced overlays	57
Table 14.	EFRON analysis of I-271	58
Table 15.	EFRON analysis of Rochester International Airport	58
Table 16.	Requirements for fabrics	63
Table 17.	Description of input data	79

CHAPTER I
INTRODUCTION

The use of fabrics in asphaltic concrete overlays for reinforcement in an attempt to prevent reflection cracking has developed into a major research area. Fabrics have been used extensively in both highway and airport pavements during the past few years. Most of the experiments in the use of fabric membranes in asphaltic concrete overlays have been with non-woven fabrics made of synthetic fibers primarily because of lower cost for non-woven versus woven fabrics. Volume I of the "Mechanistic Methodology for Airport Pavement Design with Engineering Fabrics" dealt with the research findings of non-woven fabrics of three types and described the development of a design method with a User Guide and guidelines for development of the input parameters required. Volume I documented the research efforts of the first phase of this study [1].

This research report, which is Volume II of the study, deals with the evaluation of another type of non-woven fabric membrane made of asphalt cement, fibers and stone chips. The testing of this fiber asphalt membrane is included in this phase in order to advance the technology beyond that developed in phase I. This research also covers the "Field Verification" of fabrics already used in overlays of runways and taxiways, testing requirements of non-woven fabric membranes for use in asphaltic overlays, and construction methods. Also discussed in this report is a newly developed viscoelastic model for the analysis of thermally induced reflection cracking. This model, computer coded in a program called RECK, is applicable to both field pavements and laboratory beams.

This new crack prediction model represents an advancement of the theory discussed in Volume I; it is based entirely on fundamental material properties (such as creep modulus, indirect tensile strength, and fracture toughness) and does not require the use of a distress function. The model has been validated on

one airport and four highway projects; the agreement between predicted and actual performance for these projects is very good.

This report is divided into the following major sections:

CHAPTER I:	Introduction
CHAPTER II:	Laboratory Testing
CHAPTER III:	Data Analysis, Methods and Models
CHAPTER IV:	Field Evaluation
CHAPTER V:	Specifications for Material Properties, Testing Procedures, and Construction Methods
CHAPTER VI:	Conclusions and Recommendations

Chapter II deals with sample preparation and laboratory testing at two temperatures, for fatigue and thermal stresses. Chapter III deals with the analysis of the laboratory test data. Chapter IV discusses the field evaluation of fabric performance at the Rochester International Airport and at four highway projects located in New York and in Ohio. The testing methods and construction procedures for fabrics to be used in the reduction of reflection cracking are discussed in chapter V, and chapter VI deals with conclusions and recommendations.

CHAPTER II
LABORATORY TESTING

2.1 Types of Testing

Phase I (described in Volume I of this report) presented test data conducted on three non-woven fabrics commonly used in controlling or minimizing the phenomenon of reflection cracking [1]. The use of a fiber-reinforced asphalt interlayer has shown some promise for this purpose also. Therefore, the fiber-reinforced interlayer has been included in phase II activities in order to advance the information beyond that in phase I.

This study is concerned with the evaluation of the cracking resistance of fiber reinforced asphalt concrete overlays of rigid (portland cement concrete) pavements. In order to evaluate the cracking resistance of the fiber reinforced system, tests were conducted under the following conditions at two temperatures:

1. Fatigue resistance under load of asphalt overlays over concrete bases for both control and membrane reinforced conditions. Control conditions are conventional overlays without fabric reinforcement. Tests on control specimens were performed during phase I study [1].

2. Horizontal and vertical temperature induced stresses for both control and membrane reinforced overlays.

The beam testing simulates full scale flexible pavement overlay behavior under aircraft load as experienced in runways and taxiways. Figure 1 illustrates the concept for an overlay condition. Membrane reinforcement involves placement of an engineering fabric or geotextile underneath the asphalt overlay. The purpose of membrane reinforcement is to enhance the fatigue crack resistance of the bound layer. Simulation of reflective cracking of rigid pavement overlays requires modeling of both

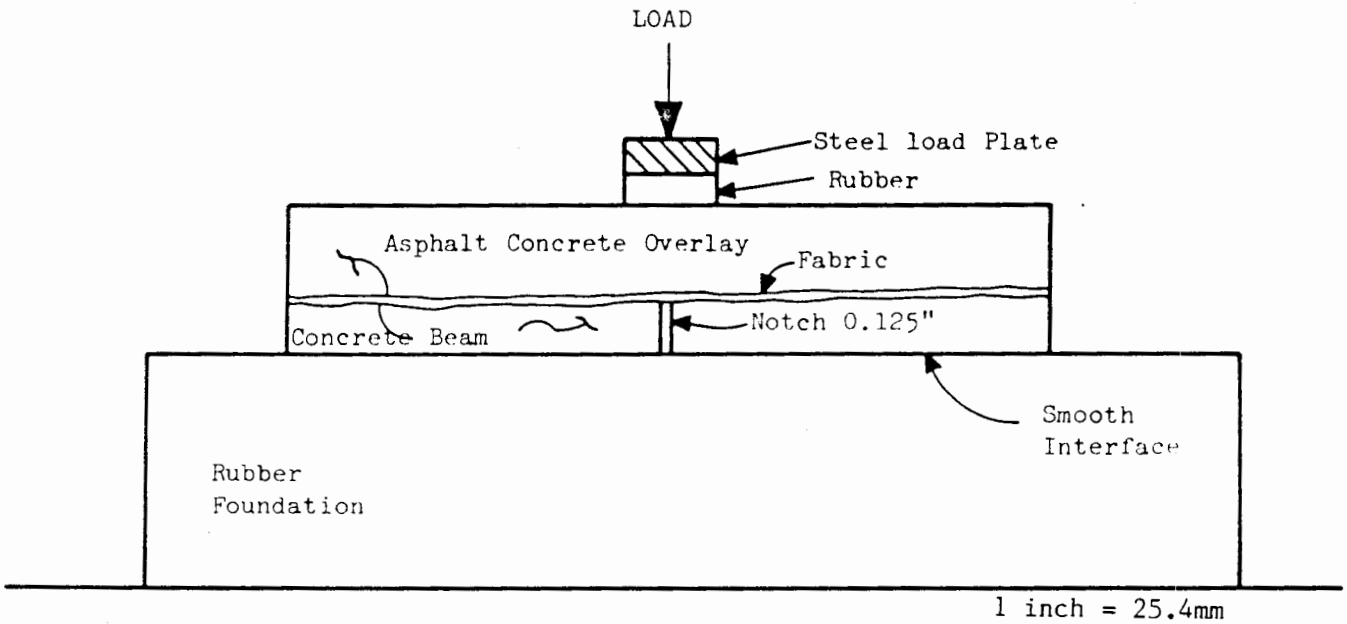

Figure 1 FATIGUE TEST SET-UP

thermal and traffic loading conditions. Thermal stresses result from both seasonal and daily changes in slab temperature. The thermal loading can be represented by the superposition of two different thermal conditions.

a. Uniform change in slab temperature: this condition represents the seasonal changes in average slab temperature which occur over long periods of time.

b. Pure curling condition: daily, or short time period, temperature variation within the slab. For pure curling the average slab temperature remains unchanged but the upper surface of the slab is at a different temperature from the lower surface with the temperature assumed to be linearly related to the slab depth.

Manufacturing full scale pavement models and subjecting them to actual thermal loads experienced in the field was neither economically feasible nor possible given the time constraints of this study. Therefore model pavements with external forces applied to produce joint movements equal to those of full scale pavements under field thermal loading were designed. Uniform seasonal reduction in slab temperature was simulated by applying horizontal tensile forces to the model pavements. Traffic forces were simulated by applying dynamic vertical loads to the model which was a beam supported on an elastic foundation.

2.2 Fabric Selection

Three types of engineering fabric membrane were selected initially for this study and the evaluation of their performance was indicated in Volume I of this report [1]. Subsequently one more membrane was selected for evaluation in this study; the pertinent information on the membrane is indicated below.

The selected membrane was manufactured using asphalt cement, a plasticizer, polypropylene fibers (designated by the manufacturer as Fiber 3010), and Delaware stone chips. The percent of plasticizer and fiber used in making the membrane were each 6% by total weight of the mix.

2.3 Mix Design

A brief report on the mix design of concrete used for rigid base, and mix design used for asphalt overlays are detailed in the following sections:

2.3.1 Portland Cement Concrete Beams

Two different sizes of aggregates from a local company were utilized for the manufacture of portland cement concrete beam specimens. The aggregates used were #57 crushed gravel as coarse aggregate and natural sand as fine aggregate. The aggregate gradation limits were in accordance with FAA specification P-401; actual gradation chosen for preparing the mix design is shown in figure 2. The quantities of the constituents of concrete, namely coarse and fine aggregate, cement and water, were chosen as per FAA specification for Class C concrete after making necessary adjustments for water absorbed by the dry aggregate, and for the net water requirement of concrete due to presence of water in a polymer additive. The polymer additive used was supplied by Dow Chemical Company; the quantity used was 10 gallons of additive per cubic yard (49.7 litres per cubic meter) of concrete. The polymer additive was used to obtain a higher strength concrete so that the beams could be reused. The calculated mixture proportions were checked by means of trial batches. The quantities by weight of the several constituents of regular concrete are indicated in table 1 and the aggregate gradation are shown in table 2. The slump selected was three inches (76.2 mm), entrained air 4.5% and water cement ratio of 0.45. The procedures delineated in ASTM C-192 were strictly followed for making and curing beam specimens of concrete in the laboratory.

Table 1

Polymer concrete mix data.

Cement Content	= 658 lb/C.Y.
Coarse Aggregate	= 1737 lb/C.Y. (#57 Gravel)
Absorption	= 1.2%
Specific Gravity	= 2.64
Fine Aggregate	= 1107 lb/C.Y. (natural sand)
Absorption	= 2.7%
Specific Gravity	= 2.50
Water/Cement Ratio	= .40
Polymer Additive	= 10 gal./C.Y. (manufactured by Dow Chemical Co.)
Percent Entrained Air	= 4.0
Slump	= 3"
Compressive Strength (28 days)	= 4800 psi

Table 2

Gradation limits of aggregate.

#57 Lime Stone		Natural Sand	
Sieve Size	% Passing	Sieve Size	% Passing
1/2"	100	3/8"	100
1"	95-100	#4	95-100
1/2"	25-60	#8	70-100
#4	0-10	#16	45-80
#8	0-5	#30	25-60
		#50	5-30
		#100	1-10
		#200	0-4

Note: 1 in = 25.4 mm

Molds used for casting beam specimens were made out of wood. Molds were water-tight during use, as judged by their ability to hold water. Beam molds were rectangular in shape and of the dimensions required to produce the stipulated specimens. Curing of concrete specimens was performed as per ASTM C-192. After the required period of curing, the beam specimens were sawed with a diamond blade saw to get specimens of the following size:

1.5 x 3 x 12 in (38 x 76 x 305 mm)

2.3.2 Asphalt Concrete

Two different sizes of crushed limestone aggregates from a local company were utilized for the manufacture of asphalt concrete specimens. The aggregates used were #8 crushed limestone as coarse aggregate, and limestone dust as fine aggregate. The #8 crushed aggregate generally showed sharp, angular, and gritty particles, and, for the most part, contained at least one fractured face in the particles, and were reasonably free from excessive dust or other deleterious coatings, weathered pieces, or excessive flaky and/or elongated pieces. Measured water absorption of particle size ranged from between 2.9% and 3.2%. Aggregate gradation conformed to FAA specifications for asphalt concrete surface course. Gradation ranges of the #8 crushed aggregate, based on frequent samplings, are shown in table 3. Asphalt cement (AC-20) used in this investigation was obtained from Chevron Asphalt Company. Figure 3 gives details about the aggregate gradation of #8 limestone aggregate and sand used in development of P-401 mix. Design of aggregate blends for this investigation was based on:

i. Raw material aggregates and their individual gradings

ii. General conformance with FAA specifications for P-401 mix

For mix design and investigation, five levels of binder were used, namely: 5.5, 6, 6.5, 7, and 7.5% by weight of total mix.

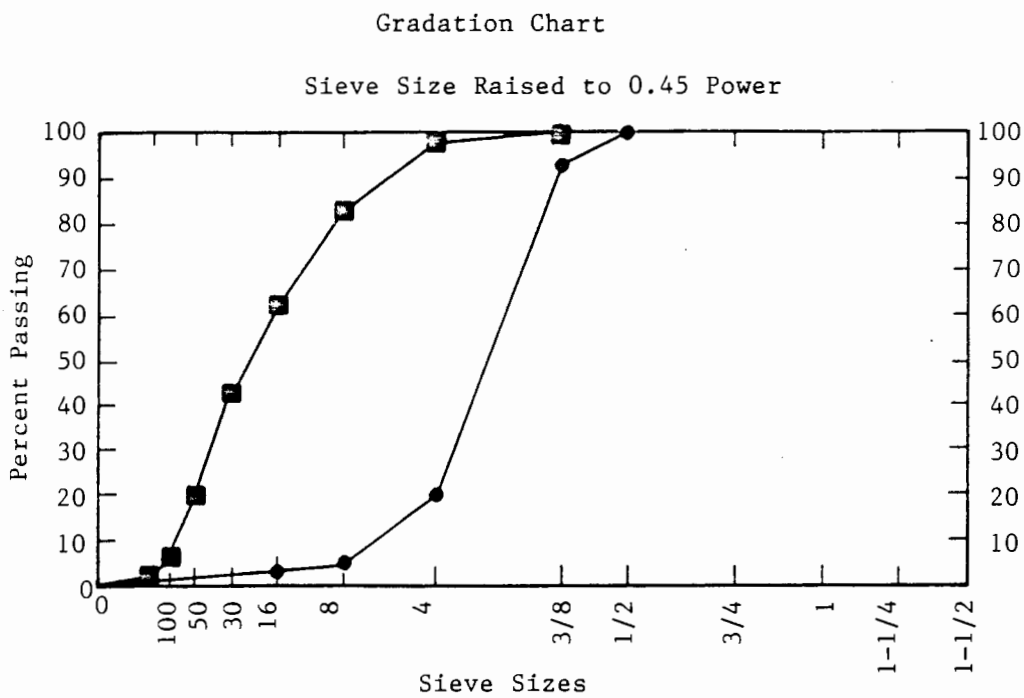

Figure 2. Gradation of Concrete Aggregate

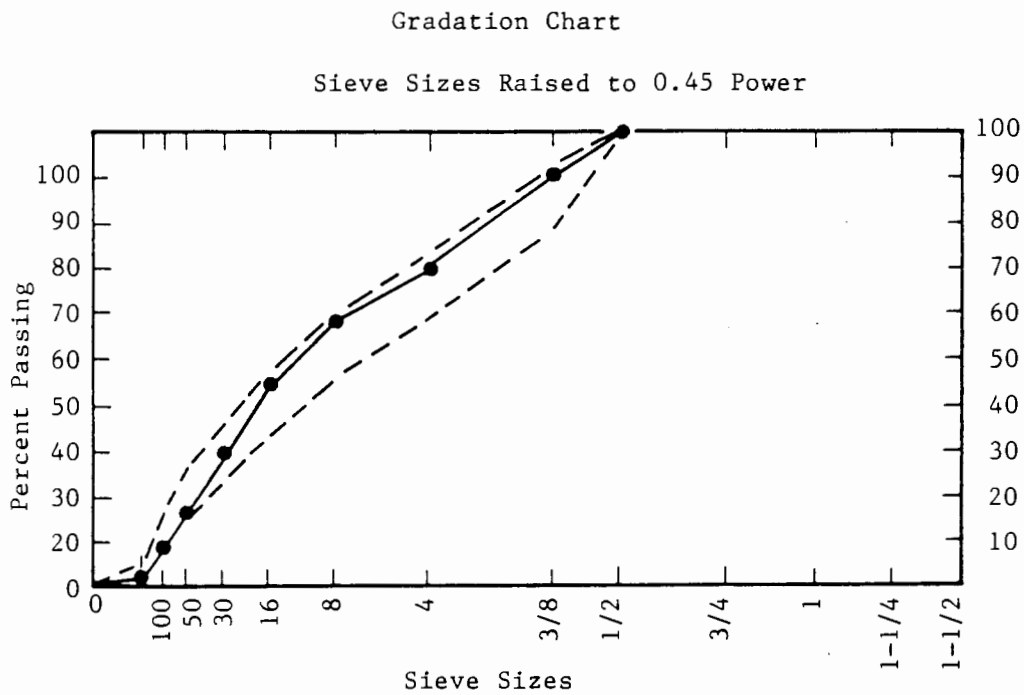

Figure 3. Gradation of P-401 Asphalt Concrete Mix

The optimum asphalt content for the selected aggregate gradation was determined using Marshall design procedures and 75 blows/face compaction efforts. Optimum asphalt content was determined as the average of asphalt content for optimum stability, density, and 4% air voids. The Marshall mix design properties for this mix are presented in figure 4.

Table 3
Gradation of P-401 asphalt concrete.

Sieve Size	Percent Passing	FAA Gradation Limits
1/2"	100	100
3/8"	91	79-93
#4	70	59-73
#8	58	46-60
#16	45	34-48
#30	30	24-38
#50	17	15-27
#100	9	8-18
#200	3	3-6

Note: 1 in = 25.4 mm

2.4 Sample Preparation

Specimens for testing were of the following types:

1. 1.5 in (38 mm) thick base portland cement concrete beam, notched with teflon strip in the notch, overlaid with 2 in (51 mm) thick asphalt concrete. The concrete beam had tack coat with SS-1h at the rate of 0.15 gallon per square yard (0.68 liter per square meter).

MARSHALL MIX DESIGN

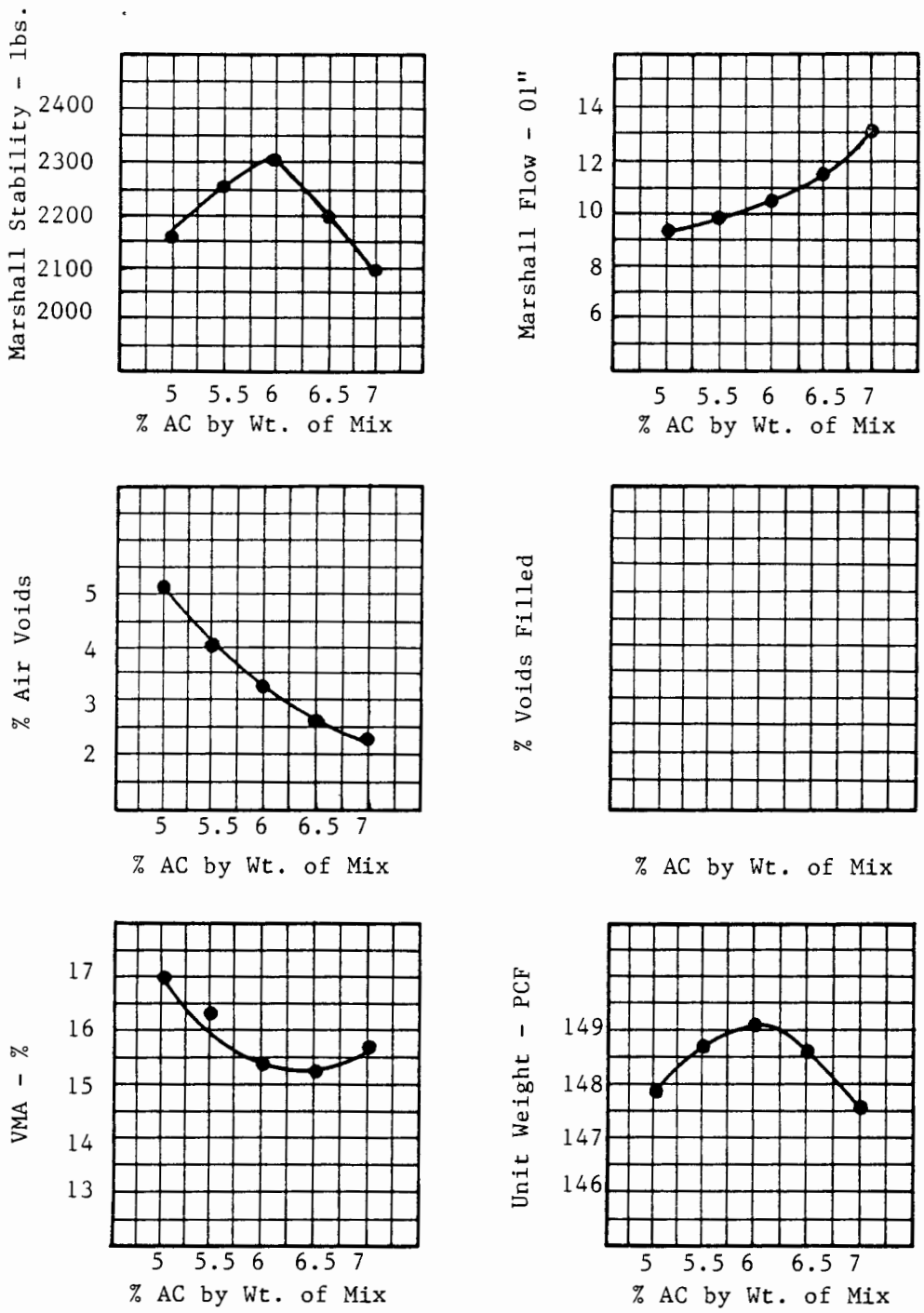

Figure 4. Marshall mix design data for P-401

FAA WJH Technical Center
00093439

2. Same as above with a reinforced membrane placed on the tack coat, before the AC overlay

3. Same as (1) above but using 3 in (76 mm) thick overlay

4. Same as (2) above but with 3 in (76 mm) thick overlay

For the membrane reinforced beams, the lower part of the specimen was first manufactured with concrete as a beam of size 1.5 x 3 x 24 in (38 x 76 x 610 mm) and then sawed into two parts. Tack coat with SS-1h was applied over the concrete beam and then the fabric membrane was placed over the sticky tack coat material. Care was taken to maintain a 1/8 in (3 mm) separation between the saw-cut pieces during fabric placement.

After the placement of fabric on the top of tack coated base beam the fabric surface was brushed to smooth the fabric and to bring it into complete contact with the binder. The base beam with tack coat and the fabric thus prepared were placed in a beam mold and a weighed quantity of hot mix (P401) poured over the beam. A wire comb was passed through the loose material back and forth for even distribution of the mixture in the mold. The mixture was then pressed under steadily increasing load until the asphaltic mixture was compacted to desired thickness (rather than a specific load) to insure that desired density would be achieved. The mold was then dismantled and the specimen was placed on a stiff support, such as a piece of wood or steel, to await testing. All precuations were taken to prevent bending and any possible damage to the beam sample prior to testing. The compacted test specimen was allowed to cool at room temperature for a minimum of 24 hours prior to testing.

2.5 Laboratory Testing

2.5.1 Fatigue Testing

The fatigue experiments were conducted using a beam on elastic foundation with geometry as shown in figure 5. The

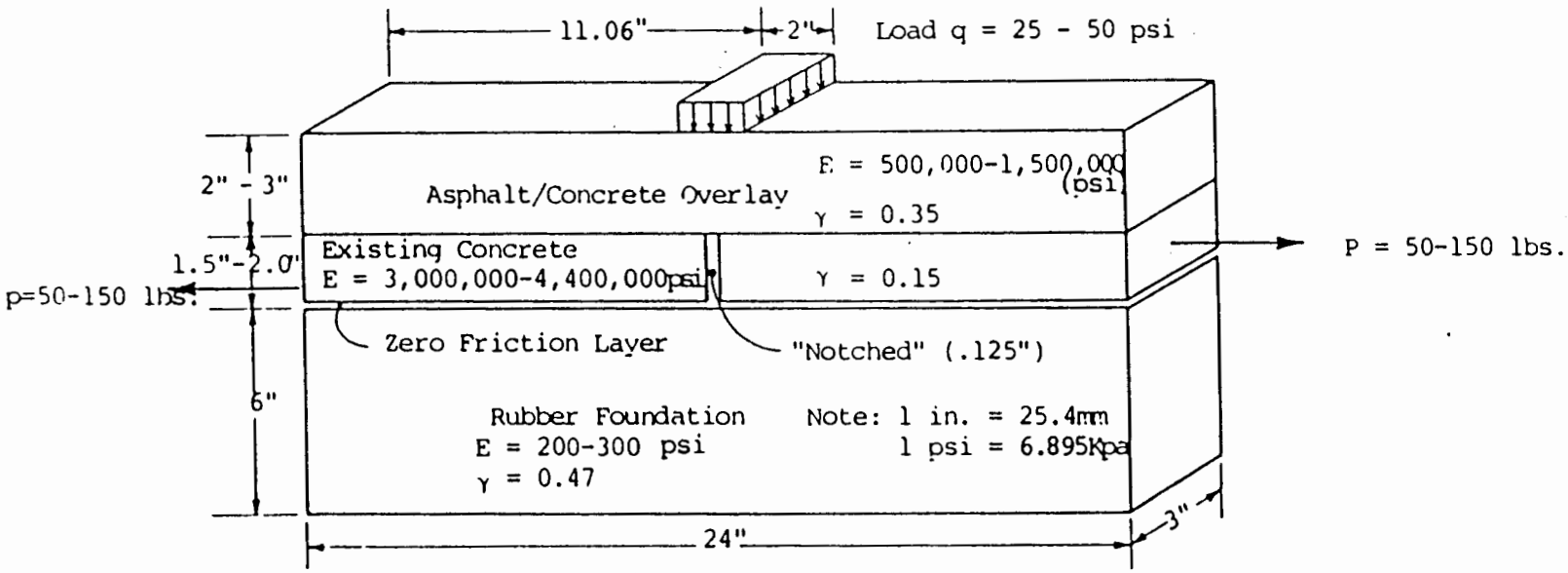

Figure 5 . Laboratory Simulation of Overlaid Concrete Pavement.

selection of this experimental set-up was based on a two-dimensional modeling of the pavement structure in which a beam representing the pavement is supported on an elastic foundation representing the subgrade. The dimensions of the beam and foundation, as well as the foundation stiffness were selected with consideration to simulating the stress and strain at the bottom of a pavement structure subjected to traffic loading. The test set-up was the same as previously used by Resource International, Inc. and researchers at the Ohio State University to study the fatigue properties of asphaltic mixtures [1,2]. The fatigue tests were performed using a dynamic load function of haversine shape. An MTS electro-hydraulic testing system was used to generate the load factor. To insure complete recovery of the sample before the next load cycle, a rest period of 0.4 seconds was allowed between each load application. The duration of load application in all tests was kept constant at 0.1 seconds. Fatigue test data of samples tested at 40 and 72 degrees F (4 and 22 degrees C) and at different stress levels are presented in appendix A.

2.5.2 Horizontal and Vertical Stresses

The test set-up is shown schematically in figure 5 and pictorially in figure 6. A constant horizontal pull was applied and the crack development in the asphalt overlay was measured with a micrometer guage. Tests were planned to be conducted until the crack developed fully in the overlay and to measure the joint opening in the concrete base, but these tests could not be carried to conclusion as the overlay debonded during the tests. The debonding phenomenon occurred at both 40 and 72 degrees F (4 and 22 degrees C), except that the debonding at 40 degrees F (4 degrees C) took place after a longer period of time. Complete test data for these specimens is therefore not available. However, the debonding of the test specimens may indicate that only limited thermally induced stresses can be developed in overlays of actual pavements that use the fiber SAMI reinforcing. The theory developed in Volume I indicates that if debonding

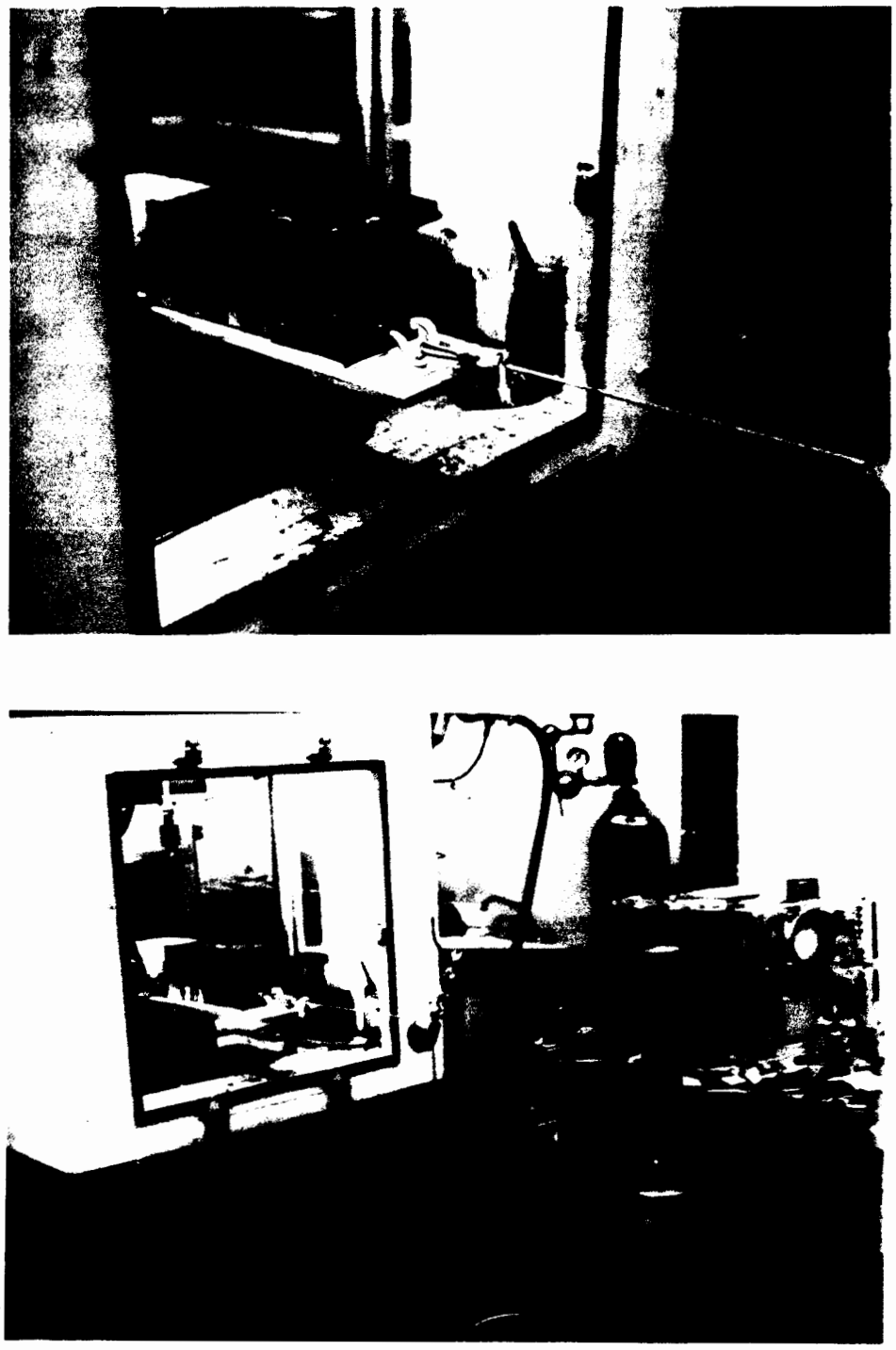

Figure 6. Test Set-up for Simulated Thermal Loads.

occurs before stresses reach critical level, thermally induced reflection cracking will not take place. It should be kept in mind that reflection cracking also develops as a result of repeated traffic loading (fatigue). However, since, as will be seen in the analysis in the next chapter, the fatigue properties of the fiber SAMI are better than for the other materials tested during phase I, this treatment shows promise as a method for minimizing the reflection cracking phenomenon. Field trials are necessary to completely verify this conclusion.

CHAPTER III
DATA ANALYSIS, METHODS AND MODELS

3.1 Fatigue Life

The fatigue testing of the laboratory beams was conducted under controlled applied load conditions. Fatigue analysis requires the determination of critical tensile strain in the asphaltic concrete and relating this strain to the allowable number of load applications; i.e., the fatigue response is given by:

$$Nf = A\,\varepsilon^{-B} \qquad (1)$$

where:

Nf is the number of load appplications to failure

ε is the critical tensile strain

A, B are material constants that are temperature dependent.

The fundamental assumption of mechanistic stress/strain analysis is that equation 1 can be used to describe the fatigue behavior of a particular material when the critical tensile strain is known, independent of how that strain is developed. All that is required is to determine the material constants (A, B in equation 1) from some simple laboratory test. Also the critical strain in the structure has to be analyzed. The analysis model described in chapter IV of reference 1 is used as the analysis method to determine the critical strains resulting from loading. The laboratory test data serve a dual purpose in this study:

1. To determine the material properties A, B in equation 1.

2. To verify the stress/strain analysis model.

The latter objective is the reason for the variable thicknesses used in fatigue testing.

The test data for the fiber SAMI reinforced beams at 40 and 72 degrees F (4 and 22 degrees C) are shown in figure 7. The critical strains have been determined using the EFRON program described in chapter IV of reference 1. As can be seen from figure 7 the regression equation fits the data points very well. There is some scatter in these data; however, the correlation coefficients (R-square) are 0.96 and 0.70 with standard errors of estimate (in terms of log Nf) of 0.097 and 0.105, respectively for the 40 and 72 degrees F (4 and 22 degrees C). Both values are better than generally reported for fatigue relationships where the only variable is applied load. The pertinent fatigue parameters are presented in table 4.

It should be noted that the slopes (the B value in equation 1) of the membrane reinforced beams (indicated by dashed lines in figure 7) are the same as the slopes (B values) obtained from regression analysis of the control beams. The fatigue data for the fiber reinforced beams were analyzed assuming linear elastic response; i.e., that the stress and strain are proportional to applied load and that the material properties are independent of stress, or that the fabric effectiveness is independent of stress level. Consequently, the fiber reinforcing must behave in the same way in the system independent of the applied load/stress level.

The fatigue data for the fiber SAMI beams are compared to control beams and other treatments in figures 8 through 11 at 40 and 70 degrees F (4 and 22 degrees C). The results of regression analysis are presented in figures 8 and 9; and it is assumed that linear elasticity is applicable (the slope of the reinforced beams is the same as the control beams) in figures 10 and 11. It is seen that the fiber SAMI performs considerably better than control and somewhat better than the other treatments at 40 degrees F (4 degrees C) and performs considerably better than both control beams and other treatments at 72 degrees F (22 degrees C), independent of the method of analysis.

Table 4

Fatigue parameters.

Temperature ^{o}F (^{o}C)	Regression Equation A	B	R^2	SE	Assuming B = Constant A	B	SE
40 (4)	2.98×10^{-1}	1.787	0.70	0.105	4.91×10^{-10}	4.425	0.354
72 (22)	1.53×10^{-8}	4.02	0.96	0.097	3.21×10^{-10}	4.558	0.129

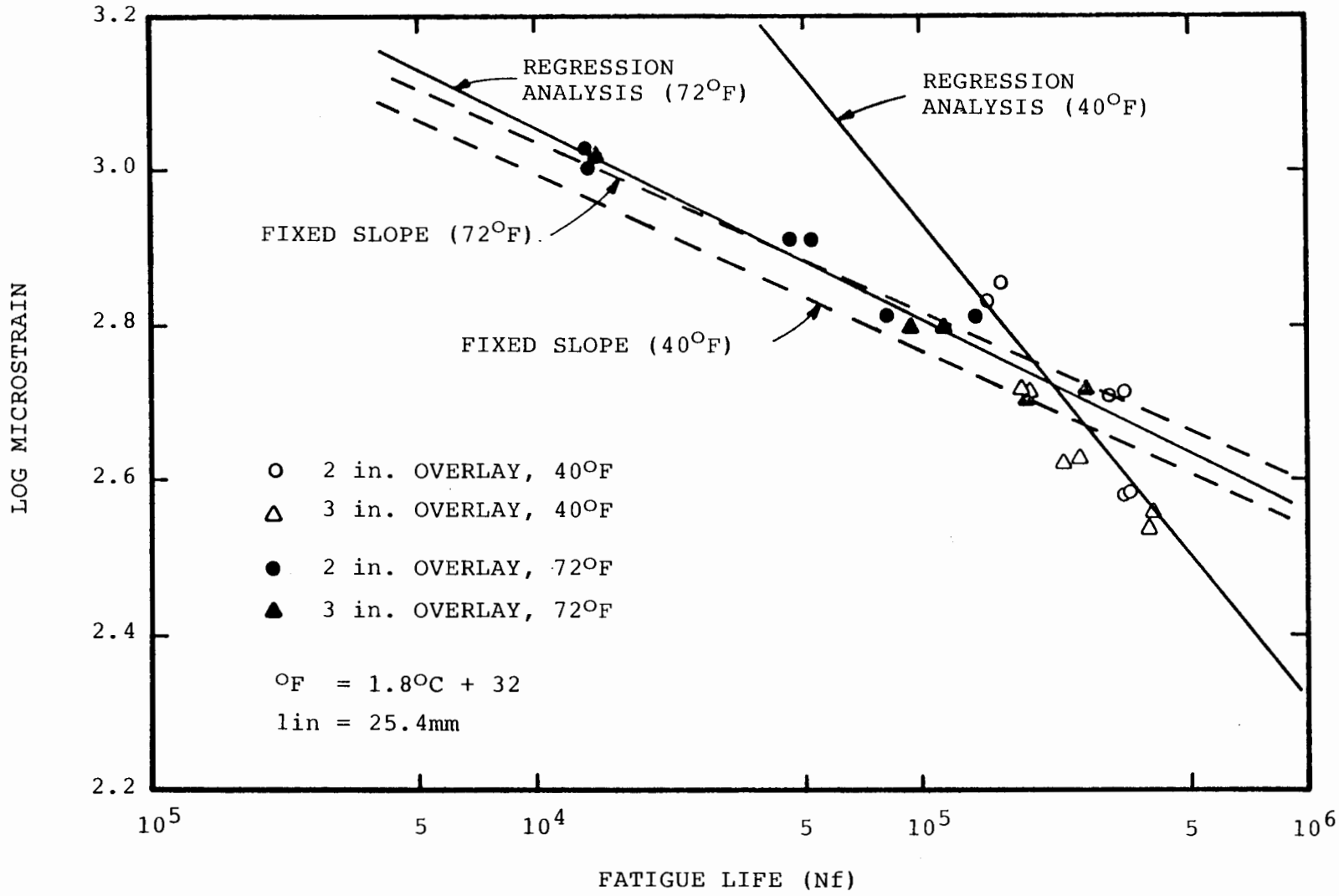

Figure 7. Laboratory fatigue data for fiber sami at 40 and 72°F.

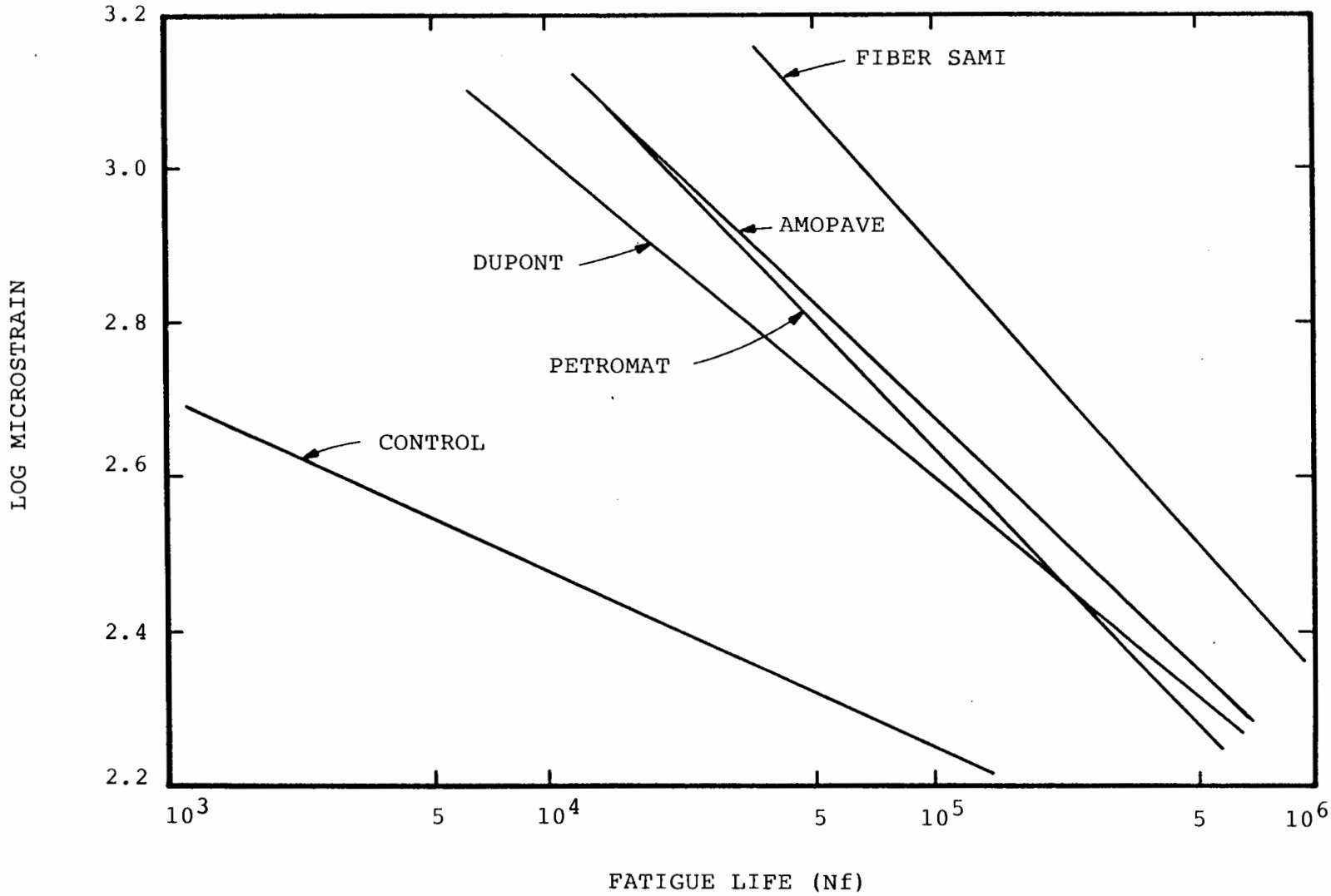

Figure 8. Comparison of fatigue lives at 40°F (4°C).

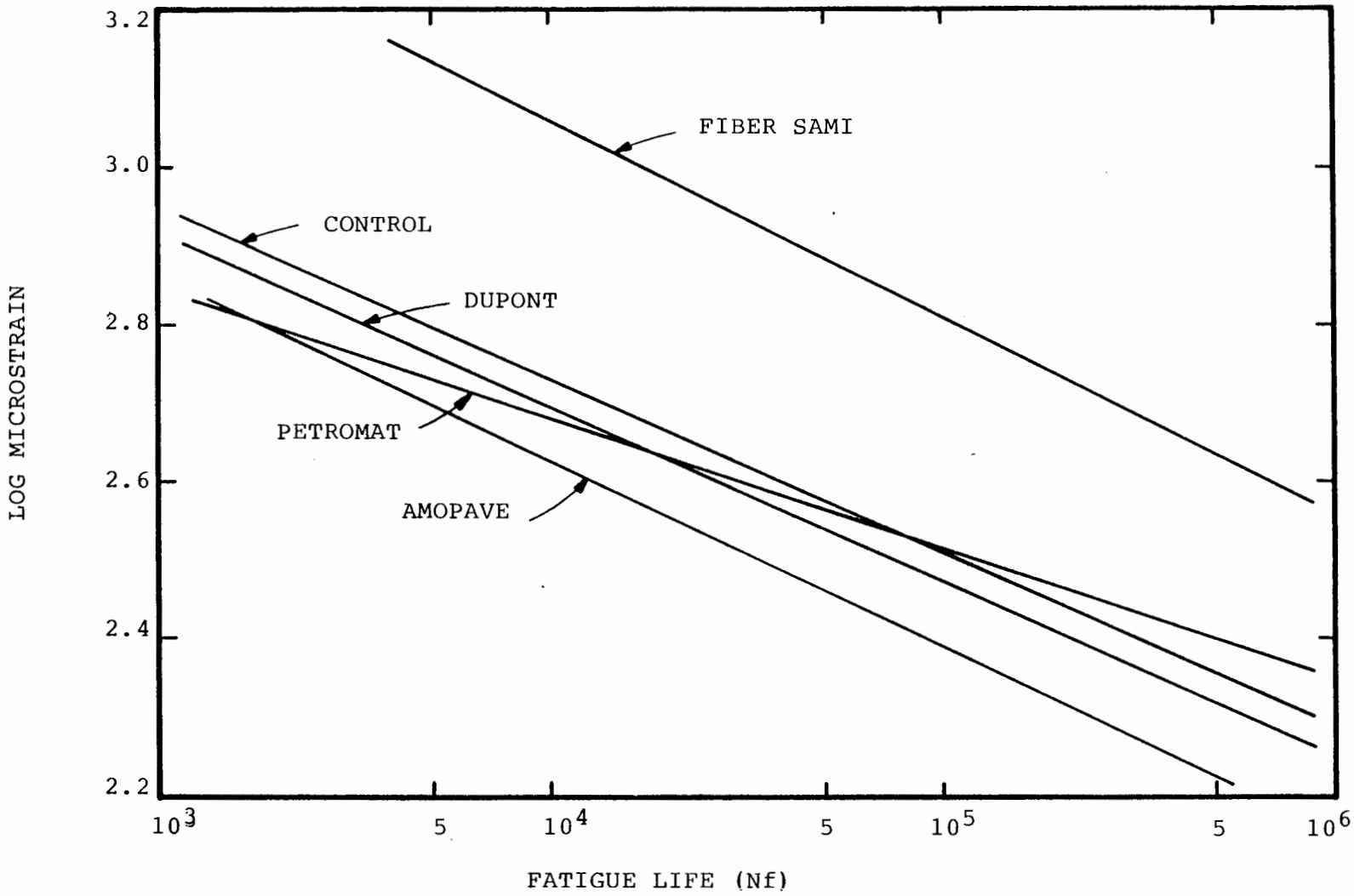

Figure 9. Comparison of fatigue lives at 72°F (22°C).

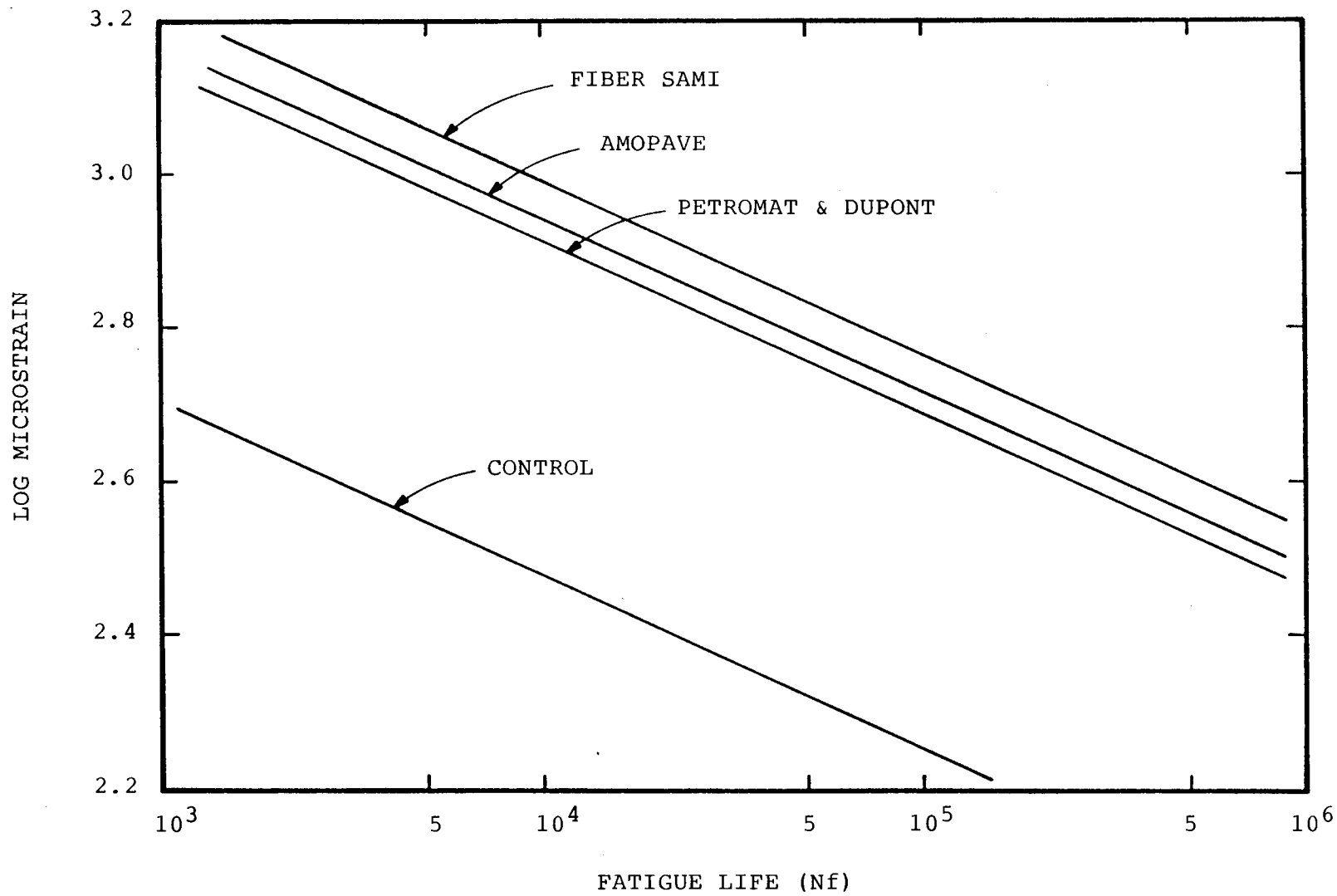

Figure 10. Comparison of fatigue lives at 40°F (4°C).

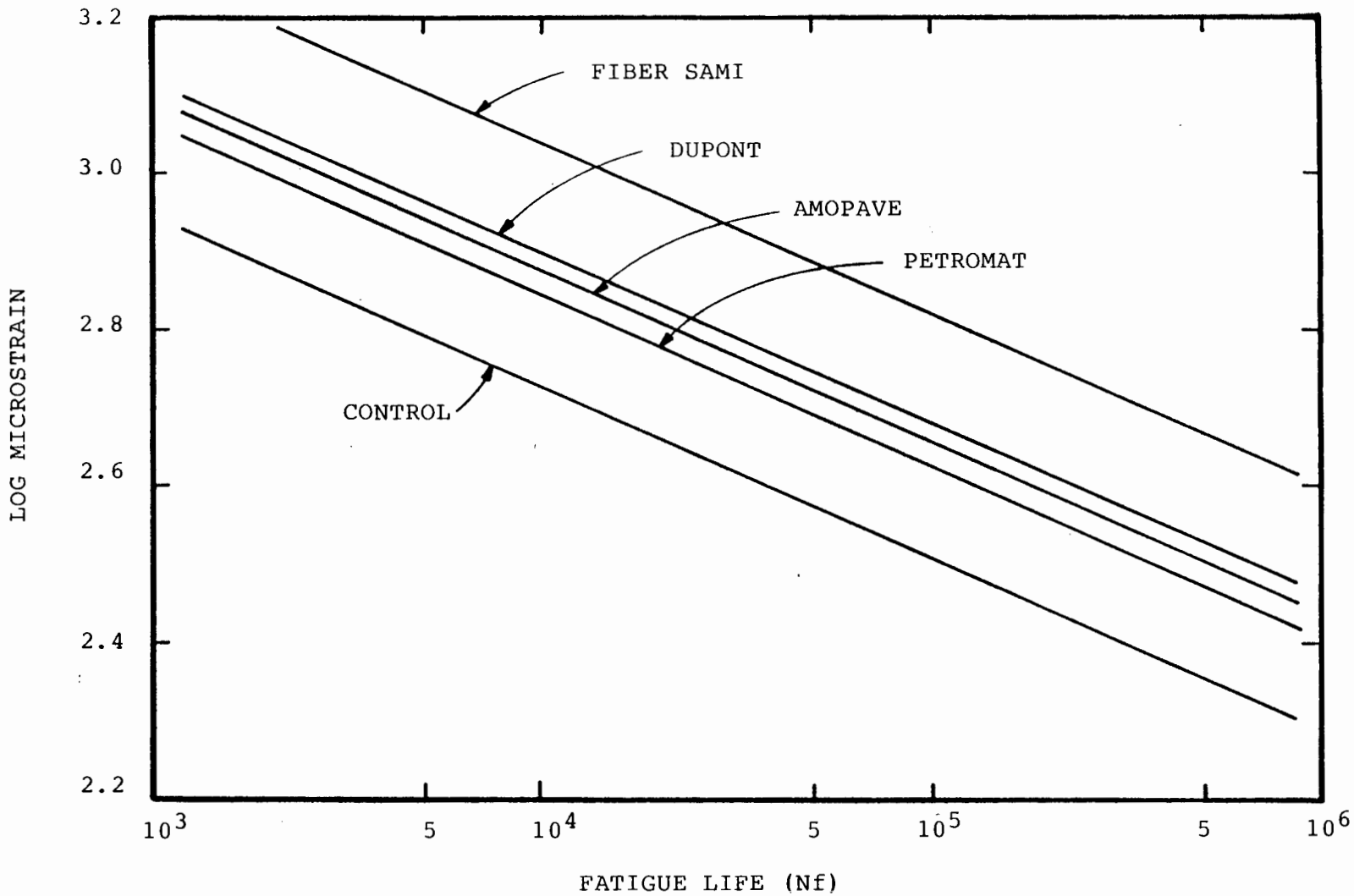

Figure 11. Comparison of fatigue lives at 72°F (22°C).

Regression analysis of the fiber reinforced fatigue data indicates that the slope at 72 degrees F (22 degrees C) is not drastically different from the control beam slope, but is substantially different at 40 degrees F (4 degrees C). This same conclusion was also reached when testing other fabric reinforced beams [1]. Thus, the assumption of linear elasticity is not entirely valid; however, non-linear elastic and/or elasto-plastic analysis is beyond the scope of this project. Furthermore, as is indicated by the standard error values in table 4, the assumptions of linear elasticity do not increase the standard error values by much - the slight loss in precision is amply compensated by the great simplification in the analysis method.

However, the regression analysis results could also be used, along with a phenomenological model, to predict the fatigue response. The disadvantage of this approach is that fatigue response cannot be predicted from fabric properties alone but would require laboratory testing. The amount of testing is not extensive, and the improved confidence level in the predicted response may outweigh the disadvantage.

As indicated above, the 40 and 72 degrees F (4 and 22 degrees C) test data are summarized in figures 10 and 11, respectively. It is apparent from figure 10 that fabric or fiber reinforcement has a significant beneficial effect at 40 degrees F (4 degrees C) but that the difference between reinforcements is rather small. Figure 11 shows that the effect of fabrics on performance at 72 degrees F (22 degrees C) is not very great, nor is the difference between fabrics; however, the fiber SAMI performs considerably better than do the other treatments. The most probable explanation for this phenomenon is that although the off-the-shelf fabric properties are different among the various fabrics, the fabric-tack coat system properties are not significantly different (the better performance of the fiber SAMI layer can be explained by the increased thickness of that layer over that for the fabric layers). Furthermore, in-situ

fabric-tack coat system properties at 72 degrees F (22 degrees C) are not very different from asphaltic concrete properties, so that fabric effectiveness in relieving stresses is not great. At 40 degrees F (4 degrees C) however, the difference between fabric system and asphaltic concrete incrases, leading to greater stress relief and fabric effectiveness. The fiber SAMI layer appears to be more effective in all cases in retarding fatigue cracking.

3.2 Development of a Mechanistic Model for Thermal Stress Analysis

A phenomenological model was developed in phase I of this study to analyze the phenomenon of thermally induced reflection cracking [1]. The model described below is based on mechanistic concepts and represents a considerable advancement over the model developed previously. The previous model utilized elastic theory whereas viscoelastic concepts are used in the new method.

In search of a mechanistic approach to the problem of reflective cracking, Schapery and others performed theoretical studies to analyze fracture of a viscoelastic material; this work seemed promising for adoption in this research [3]. Schapery, et al. have successfully applied this approach to the fracture characterization of metals [2]. In the application of this theory to asphaltic concrete, however, there is a need to employ caution in the mathematical treatment of the developed model along three lines: firstly, the simplifying assumptions do not violate the theory while at the same time realistically model the mechanics of beam fracture,; secondly, the developed model should require easy-to-find input parameters that could be obtained from the laboratory testing data to be obtained in this study; and thirdly, some modification to the model is required since this study is dealing with different materials (asphaltic mixtures and fabrics) than were used by the above cited researchers.

3.2.1 Crack Initiation and Propagation in Viscoelastic Media

To date, most of the fracture mechanics approaches assume that material behavior is either linear elastic or viscoelastic. It is further assumed that the stress field in a plane viscoelastic body subjected only to prescribed traction forces is the same as that in an elastic body of the same geometry and loading provided that the resultant force on any closed boundary vanishes. It follows as a corrolary that the stress intensity factors, K, for similarily loaded linear elastic and viscoelastic bodies satisfying this condition are equal. For an elastic material, the stress intensity factor K is independent of the crack growth rate $\dot{a}$; however, for linear viscoelastic material two cases arise: 1) for a very slowly growing crack (quasi-elastic case), the material will respond with long decade line creep compliance $J(\infty)$ being the material characterizing parameter, and 2) for a very rapidly propagating crack growth (dynamic case), $\dot{a} \to \infty$, the material will respond with the short decade time creep compliance $J(0)$ being the material characterizing parameter. Therefore, the viscoelastic stress analysis solution will not only depend upon the appropriate use of the correspondence principle but will also depend on what crack speed will develop (or can reasonably be assumed) under the specified loading conditions; i.e., quasi-elastic or dynamic analysis is used [4].

Consider figure 12 for a viscoelastic medium subjected to stresses acting along the crack plane (Mode I) in the neighborhood of a crack tip (indicated by O, and located at $x = a(t)$), where the crack plane is defined by $y = 0$. It is convenient to define a reference system attached to the moving crack tip as $r = x - a(t)$. The region $o < r < \alpha$ is termed the cohesive zone where the material exhibits non-linear material behavior (more precisely nonproportional stress/strain/time behavior). This zone was first recognized by Dugdale in his cohesive fracture model [5]. The material behavior outside this

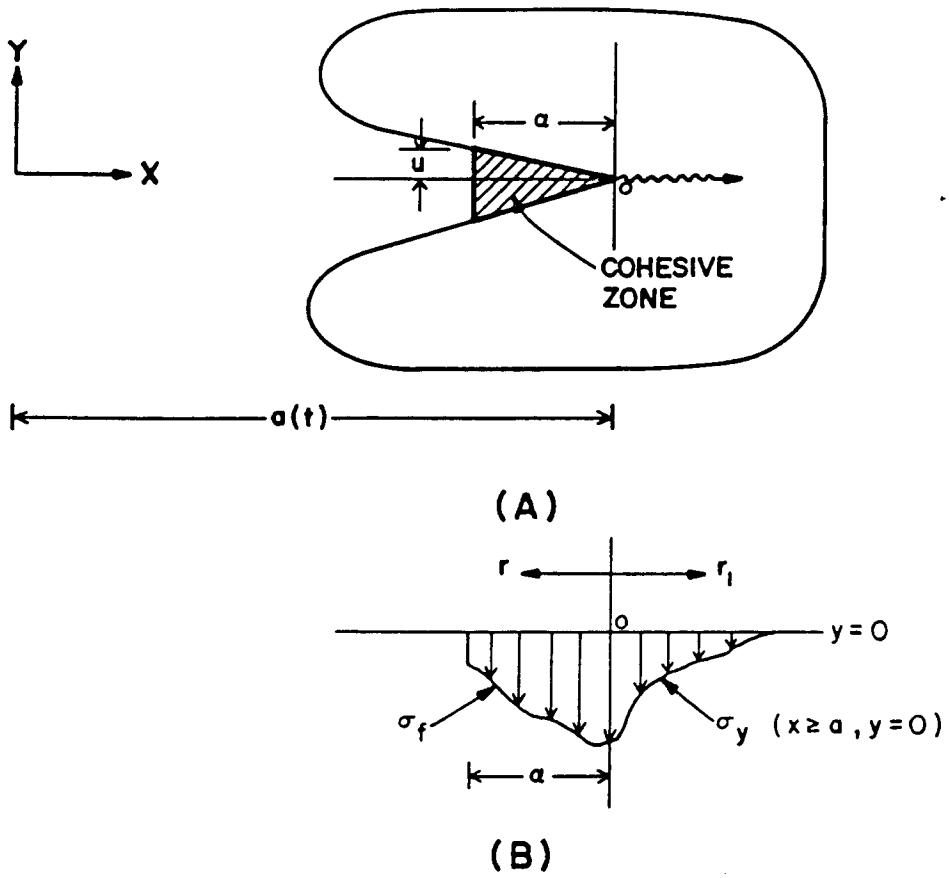

Figure 12 Crack in a Viscoelastic Medium

zone is assumed to be linear viscoelastic. The basic problem is to find the following:

1. The size of the cohesive zone, α

2. The crack opening displacement, U

3. The crack growth rate, $\dot{a}$

3.2.2 Boundary Value Problem Solution

As was indicated previously, the new analysis model utilizes viscoelastic instead of elastic formulation for the reflection cracking problem. One method for finding the solution to the viscoelastic problem is to use the correspondence principle, i.e., when a solution for the equivalent elastic problem is known, the solution to the viscoelastic problem could be found using the correspondence principle method [4]. This principle emerged from observing that the only difference between formulating a boundary value problem for a linear elastic or viscoelastic medium is in the assignment of the Young's modulus of elasticity, E and Poisson's ratio, μ. In other words, if the elastic solution exists for a boundary value problem, then the corresponding viscoelastic soltions could be found by simply replacing the material constants (E, μ, G, K) of the elastic solutions by their viscoelastic equivalents. This principle applies in the case of stationary crack; however, two conditions have to be met in order to use the correspondence principle for growing cracks. The first condition is that the cohesive stresses f are independent of the material constants. Such a requirement could be met by prescribing f a priori, as is the case in the Dugdale model [5]. The second condition is that the displacement in the plane of the crack could be expressed in separable form of two multiplicable functions; one for the material constants and the other for the geometry. Such a requirement could be met if the resultant force on any closed loop is identically zero.

It follows from the above discussion that if Ue is the elastic displacement field for a unit value of creep compliance then the corresponding viscoelastic displacement Uve could be written as:

$$U_{ve} = \int_0^t J(t-\tau) \frac{\delta Ue}{\delta \tau} d\tau \qquad (2)$$

Using the condition of small scale yielding ($\alpha << a(t)$) and considering figure 12, the elastic solution, following Dugdale approach could be written as [5].

$$\sigma_y = \frac{H(r_1)}{2\pi r} [K - \int_0^\alpha (\sigma_f(\zeta)/(\sqrt{\zeta})d\zeta] \; ; \quad r_1 > 0 \qquad (3)$$

$$U_y = 4KH(r)\sqrt{r/2\pi} - \frac{2}{\pi} H(r_1) \int_0^\alpha \sigma_f(\zeta) \ln \frac{\sqrt{\zeta}+\sqrt{r}}{\sqrt{\zeta}-\sqrt{r}} d\zeta \; ; \; r \to 0 \qquad (4)$$

The requirement that the stress σy be non-singular at the crack tip ($r = 0$) will yield:

$$K = \sqrt{\frac{2}{\pi}} \int_0^\alpha \frac{\sigma_f(\zeta)}{\zeta} d\zeta \qquad (5)$$

Substituting equation 5 in equation 4 will yield

$$U_y = \frac{2H(r)}{\pi} \int_0^\alpha \sigma_f(\zeta) \; 2\sqrt{\frac{r}{\zeta}} - \ln \frac{\sqrt{\zeta}+\sqrt{r}}{\sqrt{\zeta}-\sqrt{r}} d\zeta \qquad (6)$$

where

σ_y = The crack plane stress

$H(r)$ = unit step function

σ_c = stress in the cohesive zone

ζ = dummy variable

U_y = crack opening displacement

K = stress intensity factor

α = size of the cohesive zone

3.2.3 Determination of the Cohesive Zone Size, α

To meet the first condition of the correspondence principle, the cohesive stress, σf has to be predetermined. Assuming that $\sigma f = \sigma fmax\phi(r)$ where $\sigma fmax$ is the maximum value of σf (i.e., the indirect tensile strength) and $\phi(r)$ is a multiplication function evaluated at any point at a distance r from the crack tip; the size of the cohesive zone, α could be found by substituting the above into equation 5.

$$K = \sqrt{\frac{2}{\pi}} \int_{o}^{\alpha} \frac{\sigma_{fmax}\phi(r)}{\zeta} d\zeta \qquad (7)$$

Making the change of variable $\eta^2 = \zeta/\alpha ; 2\eta d\eta = d\zeta/\alpha$

Then $\zeta \rightarrow 0$ implies that $\eta \rightarrow 0$

and $\zeta \rightarrow \alpha$ implies that $\eta \rightarrow 1$

Substituting these in equation 7 yields:

$$K = \frac{2}{\pi} \int_{o}^{1} \frac{\sigma fmax\,\phi(r)}{\eta\,\alpha} * 2\eta\alpha\, d\eta \qquad (8)$$

Squaring both sides and rearranging terms:

$$K = \frac{\pi}{8} \frac{K^2}{\sigma_{fmax}^2 I^2} \qquad (9)$$

where:

$$I = \int_{o}^{1} \phi(r) d\eta \qquad ; \quad 0 \leq I \leq 1$$

3.2.4 Determining the Viscoelastic Displacement, Uve

Using the correspondence principle (typified by equation 2) as applied to the elastic crack opening displacement Uy in equation 6 yields:

$$U_{ve} = \frac{8}{\pi}\,\sigma_{fmax}$$

$$\cdot \int_{t_1}^{t} J(t-\tau)\frac{\partial}{\partial\tau}\sqrt{a(\tau)-x} - \left[\frac{\alpha+\chi-a(\tau)}{2}\ln\frac{\sqrt{\alpha}+\sqrt{a(t)-x}}{\sqrt{\alpha}-\sqrt{a(t)-x}}\right] d\tau \quad (10)$$

where $t \leq t_1$; and t_1 is the time at which the crack tip reaches the generic point x; i.e., $\zeta(x,t) = a(t) - x = 0$. Although not explicity shown in the above equation, x and σf may also be time dependent.

It follows from equation 10 that the viscoelastic displacement could be obtained if the quantities ($\sigma fmax$), J(t), and α are determined. Be reminded that for a constant cohesive stress, α depends only on the stress intensity factor K. Therefore, if information on the creep compliance J(t), fracture strength $\sigma fmax$, and the stress intensity factor K could be determined experimentally or from field measurements, then equation 10 establishes a relationship between the crack opening displacement in a viscoelastic material, crack length as function of time a(t), and the time at any specified crack length.

3.2.5 Determination of the Failure Time

Equation 10 is valid within two time bounds, t_1 and t. The lower bound t_1 defines the time required to initate a crack and advance its tip to a point $x = a(t_1)$. It is worth mentioning that Schapery indicated that the time t required to propagate the crack the distance α is approximately three times the initiation time. The upper bound t defines the time required to advance the crack or equivalently increase the crack opening displacement any specified length. At the time of rupture, the crack opening displacement reaches a critical value, Uc, and the time elapsed is defined as the failure time, tf. The work of fracture, γ, of an element in the cohesive zone until rupture occurs could be expressed by:

$$\gamma = \frac{1}{2} \int_{t_1}^{t_2} \sigma_f \frac{\delta U_y}{\delta t} \, dt \tag{11}$$

or equivalently, using change of variables, as:

$$\gamma = \frac{1}{2} \int_{o}^{c} \sigma_f \frac{\delta U}{\delta r} \, dr \quad ; \quad \dot{a} > o \tag{12}$$

where: C is the crack length at failure

if $\sigma f = \sigma$ is constant, then equation 9 reduces to:

$$\gamma = \frac{1}{2} \sigma U_c = \frac{1}{2} \sigma \Delta t_f \tag{13}$$

where: Uc is the initial joint opening displacement at failure

If the creep compliance of the asphaltic overlay could be written in the form:

$$J(t) = J_0 + J_2 t^m \tag{14}$$

then using equation 10, 13, 14 and making the change of variables $S = a(t-t)/\alpha$ will lead to the following equation for the crack growth rate, $\dot{a}$:

$$\dot{a} = \frac{\pi}{8} \left[\frac{J_2 I}{2\gamma(1 - (K/K_\infty)^2)} \right]^{1/m} \frac{K^{2+2/m}}{\sigma_y^2} \tag{15}$$

where

$$I = \frac{1}{2} \int_{1}^{o} S^m \ln \frac{1 - 1-S}{1 + 1-S} \, dS \tag{16}$$

and

J_0, J_2, m = creep compliance constants

K, K^∞ = initial and unbound stress intensity factors

Equation 15 is the general equation for the crack opening rate (the derivation of this equation is given in reference 5); however, the parameter measured in the laboratory tests is the time of failure at a specific joint opening rate. It is therefore convenient to rewrite this equation to yield the failure time, tf.

The work of fracture 2γ, required to produce a unit of surface area is given by:

$$2\gamma = J_0 K_\infty^2 \tag{17}$$

Introducing equation 17 into equation 15 and rearranging terms yields:

$$\frac{da}{dt} = \frac{\pi}{8\sigma_f^2}\left(\frac{J_2 I}{C_o}\right)^{1/m}\left(\frac{K^2}{K_\infty^2 - K^2}\right)^{1/m} K^2 \quad \text{or}$$

$$dt = \frac{8\sigma_f^2}{\pi}\left(\frac{J_o}{J_2}\right)^{1/m}\left(\frac{K_\infty^2}{K^2} - 1\right)^{1/m} \frac{1}{K^2}\, da \tag{18}$$

Integrating both sides yields:

$$\int_{t_o}^{t_f} dt = \frac{8\sigma_f^2}{\pi}\left(\frac{C_o}{C_2 I}\right)^{1/m} \int_{a_o}^{a_\infty}\left(\frac{K_\infty^2}{K^2} - 1\right)^{1/m} \frac{1}{K^2}\, da \tag{19}$$

$$t_f = t_o + \frac{8\sigma_f^2}{\pi}\left(\frac{Co}{C_2 I}\right)^{\frac{1}{m}} \int_{ao}^{a_\infty}\left(\frac{K_\infty^2}{K^2} - 1\right)^{\frac{1}{m}} \frac{1}{K^2}\, da \tag{20}$$

where

t_f is the failure time

t_o is crack initiation time, assumed to be zero

a_o is the initial crack length

a_∞ is the crack length for which the crack propagation rate becomes unbounded

K is the stress intensity factor corresponding to crack length a

K_∞ is the stress intensity factor corresponding to the crack length a

I is a constant defined in equation 16

The developed model requires easy to find input parameters that could be obtained from laboratory tests. These parameters are the properties of the overlay material such as the creep compliance, J(t), the fracture strength, σf, the joint opening rate as a function of time, and the fracture toughness, KIC. The determination of KIC also requires the applied horizontal load on the beam (slab) that results in the same stresses as those developed as a result of thermal load. Other input data, required only for model verification, are measured values of the applied load, P(t), and the corresponding values of the crack length a(t), at different time intervals. Using these input parameters, the model predicts the time at which failure occurs, tf, and the crack opening displacement, U(t), at different time intervals.

In conclusion, crack propagation in viscoelastic medium is governed by two equations: equations 10 and 15. Equation 10 defines a relation between the crack opening displacement Uve, crack length a(t), and time t provided that four material parameters are known. These parameters are: the creep compliance J(t), fracture strength (σy), fracture toughness KIC, and the Mode I stresses intensity factor K. The creep compliance and the fracture strength (indirect tensile strength) can be found using test procedures detailed in the VESYS User's Manual

(reference 6) and reference 7 gives details for determining the fracture toughness and the stress intensity factor. Once the crack opening displacment-time relationship is determined, then the crack length-time relationship could be found; or vise versa.

Equation 15 defines a relationship between the crack growth rate ($\dot{a}$) and critical crack opening displacement (Uc), provided that the same material parameters of equation 10 are known. It should be noted that the critical crack opening displacement is related to fracture work by equation 13. Integrating the crack growth rate with respect to time will yield the history of crack growth and hence determining the failure time tf. The above models have been computerized in a program called RECK and the listing is found in appendix A. The use of the above computer program will enable the prediction of the critical crack opening displacement Uc, and the time required until failure occurs, tf, as a result of thermal loads. It should be noted that the analysis due to vertical temperature gradients is identical to that described above; except that the creep compliance values corresponding to 12-hour loading cycles is used. The model is applicable to both laboratory specimens and field pavements; the laboratory tests use the mechanically induced joint opening as a function time as an input parameter whereas for the analysis of field pavements, the thermally induced joint opening as a function of time is needed. The development of this value is discussed in the section 3.2.7.

3.2.6 Effect of Fabric on the Crack Opening Displacement and Failure Time Prediction

The inclusion of a fabric layer within the overlay pavement structure is expected to prevent or delay reflection cracking. The purpose of this fabric, as a reinforcing layer, is to physically restrain the opening movement of the crack as the joint underneath opens. As has been discussed, there are several other approaches to the reflection cracking problem, including

stress-relieving interlayers (such as SAMI), crack arresting interlayer (such as the Arkansas open-graded layer) and pre-overlay rehabilitation.

A mechanistic approach to determining the effect of fabrics or interlayers on crack growth rate is to include these layers in stress analysis; the EFRON program is capable of handling up to 5 such interlayers (which may be of any width). The difficulty with this approach is that the in-situ properties of the interlayers (creep modulus, Poisson's ratio, tensile strength, fracture toughness) are very difficult to determine. It had been hoped that these properties could be deduced from the results of fatigue tests; however, the analysis of small scale beam data in reference 1 showed that this is not possible within an elastic system - it was shown in that study that the interlayer properties would have to be a function of the applied stress as well. Therefore an empirical approach is used here to include the effect of interlayers; namely, the analysis is conducted assuming that the interlayers (fabric or SAMI) are not present and comparing the predicted failure time with the actual failure time to obtain a fabric effectiveness factor.

3.2.7 Analysis of Field Pavements

As was discussed previously, daily variation of temperature gradients and the seasonal variation of average pavement temperature result in changes in the joint opening; i.e., in Uve, the crack opening displacement. This displacement can be calculated using the EFRON program provided that the rate of change of temperature (average or curling gradient) is known. Thus, the field case is identical to the laboratory beam case with the exception that the load developed as a result of the temperature drop will have to be computed using EFRON for the field case instead of using the measured values for the laboratory case. The load is required to evaluate the Mode I (opening mode) stress intensity factor KI. The following procedure is used to evaluate field pavements:

1. The joint opening and the resulting stress in the asphalt above the joint are determined using the EFRON program for monthly increments of temperature drop.
2. EFRON is rerun (using a load applied horizontally to the ends of the slab) in order to find the horizontal pull required to reach the same critical stress (in the asphalt above the joint) as in step 1.
3. The results of step 1 and 2 computations are input into the RECK program and the incremental crack growth is determined. The application of this procedure is illustrated in chapter IV.

3.3 Laboratory Thermal Stress Tests

An attempt was made to test the membrane reinforced beams under simulated thermal stress, but the tests could not be completed due to debonding of the overlay. In all 6 beams were tested at room temperature and at 40 degrees F (4 degrees C) in this mode; all debonded before any distress was visible in the asphalt overlay. However, in order to illustrate the theory, the specimens tested as part of phase I of this study were analyzed with the model described in section 3.2 and its subsections [1]. The results of this analysis are presented in appendix B.

To further illustrate the use of the theory, the large scale beams from reference 6 were also analyzed. These series of tests were intended to simulate the effect of seasonal temperature drop on joint opening and crack formation. The test setup consisted of the beam being pulled apart at a constant rate and observing the joint opening, developed load and crack propagation as a function of time. The test results (time to failure) for the large-scale beams are plotted as a function of the asphaltic concrete cross section (beam width times overlay thickness) in figure 13 [8]. The solid lines represent the best fit lines through the data points with the constraint that the lines must go through zero. The equations of the regression lines along

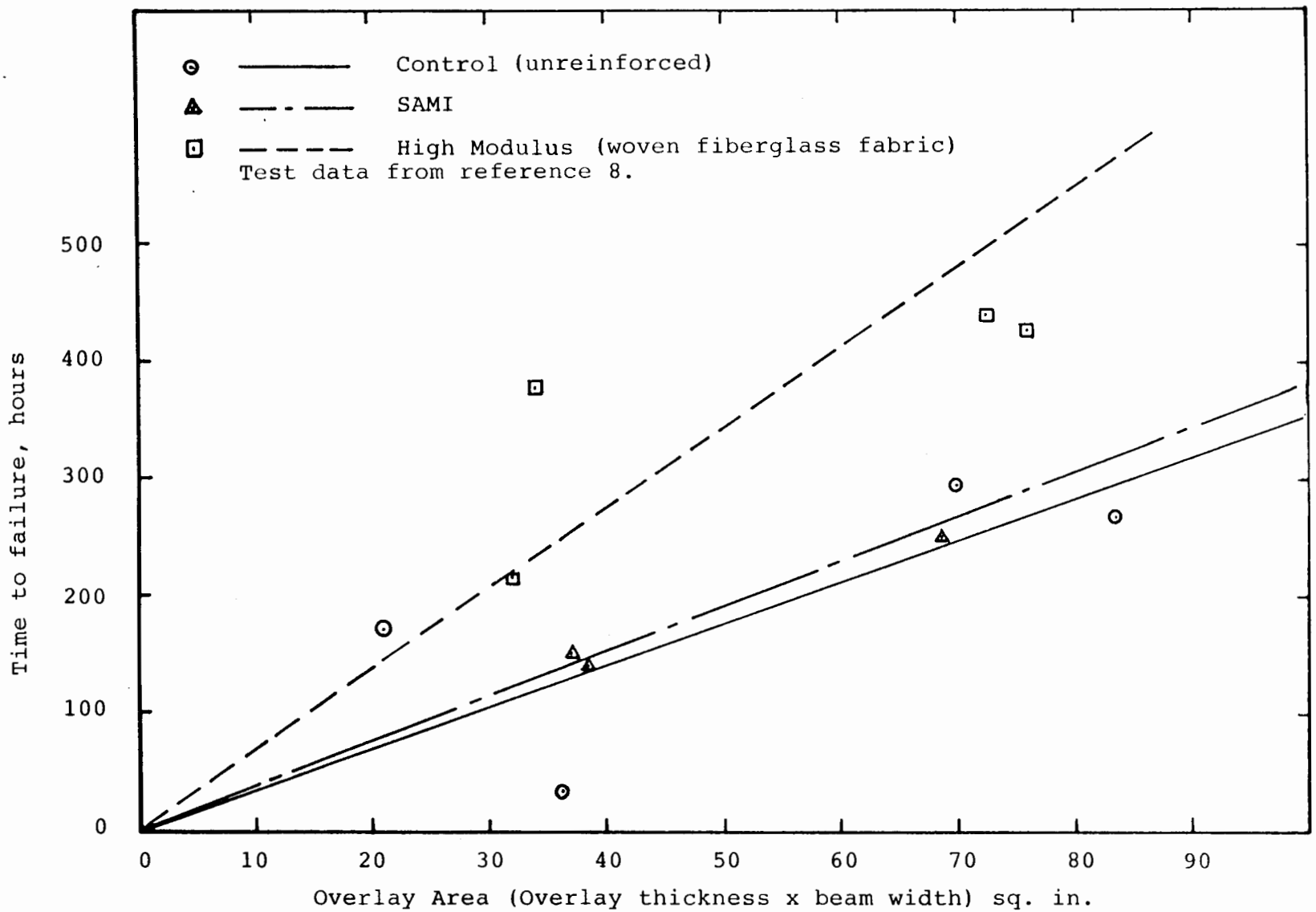

Figure 13 Results of Horizontal Pull Tests.

with the root mean square error are also shown in this figure. Although there is scatter in the data, it is apparent that the high modulus fabric (a woven fiberglass mat) increases the time to failure significantly (1.95 times) whereas the fiber SAMI material (points H) appear to have a very small effect - the effectiveness from this analysis is about 1.08. (The fiber SAMI used in reference 6 study is somewhat different from that used in this research in that the stone chip layer was absent in the former study). When considering the scatter in the data, the effectiveness of 1.08 is not significant. It is, however, encouraging that this effect is beneficial (greater than one) rather than detrimental.

The model developed in the previous section was also applied to these data. Equation 20 (computer coded as the program RECK) was used to predict the time to failure from the following input information:

1. Joint opening vs time

2. Developed load vs time

3. Test temperature

4. Creep compliance

5. Modulus of resilience

6. Indirect tensile strength

7. Fracture toughness

(the first three items were measured for each test; the remaining variables were determined from laboratory tests of the mix). It should be pointed out that the analysis of failure time assumes that the creep compliance can be expressed as:

$$J(t) = J_o + J_1 \; t^m \tag{21}$$

As discussed previously, the in-situ fabric properties are not known; therefore the analysis was conducted assuming that the fabric had the same properties as the overlay. Thus, if the prediction model (RECK) is successful and if the fabrics have a beneficial effect, the predicted failure time should agree with the actual failure time for the control samples, and should be lower by the fabric effectiveness factor for the treated specimens.

The results of this analysis are shown in table 5. The significant values in this table are under the column heading T/T'; i.e., the ratio of actual failure time to the predicted failure time. It can be seen that these data are remarkably consistent (the results for the control beam have somewhat greater scatter but the average of the two outliers is close to that of the other two results) and the fabric effectiveness, as measured by the time ratio, is close to that obtained from figure 13. Although the RECK model seems to under-predict the time to failure by about 10 percent (this is partly due to the fact that the program considers failure to occur when the crack length reaches 90 percent of the overlay thickness (the stress indensity factor becomes unbounded at the surface)), the agreement with the measurements is very good.

Table 5

Results of horizontal pull tests.

Sample No.	Width in (mm)	Hov in (mm)	Lab T Hrs	Pred T' Hrs	T/T'
9C	14.2 (361)	5.89 (149)	265.0	241.3	1.098
10C	14.0 (356)	5.00 (127)	295.0	212.3	1.390
21C	14.0 (356)	2.00 (51)	171.0	152.9	1.118
45C	14.5 (368)	2.50 (64)	31.0	44.8	0.692
6H	13.8 (349)	5.00 (127)	250.0	225.4	1.109
13H	14.0 (356)	2.75 (70)	143.5	127.8	1.115
14H	13.8 (349)	2.68 (68)	150.0	131.2	1.144
7O	14.5 (368)	5.00 (127)	440.0	238.7	1.843
8O	14.3 (363)	5.30 (135)	424.0	235.2	1.803
17O	14.0 (356)	2.30 (58)	217.0	119.0	1.824
18O	14.0 (356)	2.43 (62)	379.0	206.9	1.832

C Control

H SAMI

O High Modulus Fabric

As further verification of the developed model, the test data from phase I was also analyzed [1]. The test conditions for these tests were somewhat different - the test used 2 and 3 inch (51 and 76 mm) thick conventional (unreinforced) overlays of 3 x 3 x 24 inches (76 x 76 x 610 mm) concrete beams. Also, instead of applying a constant strain rate to the beams, a constant load was applied, and the crack length and joint opening were monitored. The RECK program was again used; the input data to the RECK program for these cases were the applied load and the crack length as function of time. Other pertinent information for these tests are: fracture toughness, KIC = 800 psi (5.5 MPa); indirect tensile strength, σ_y = 150 psi (1.03 MPa), and the creep compliance is:

$$J(t) = .000001\ (.25 + 5t^{.33}) \qquad (22)$$

where t is the transformed time. The output from these analyses are the predicted joint opening as a function of time, and the time to failure. Figure 14 shows a typical result, and the other data are presented in the figures in appendix B - again the agreement is excellent.

3.4 Application to Pavements

As discussed in section 3.3, two of the mechanisms contributing to reflection crack formation are thermal stresses resulting from daily variation in the vertical temperature gradient of the concrete slab, and the seasonal change in the average concrete temperature. It was shown in reference 1 that both mechanisms result in changing the joint opening, which can be calculated using the EFRON program.

The change in joint opening is the result of variation in temperature over a period of time; i.e., the rate at which the joint opening changes can be calculated if the time rate of change of temperature (either seasonal or daily temperature gradient) is known. This change in joint opening is precisely the parameter required for the failure analysis described in section 3.3 and its subsections. Thus the same theory and models used to analyze the laboratory test response to thermal loading are directly applicable to the analysis of full-scale pavements. Of course, this analysis requires certain input data such as the elastic material properties (modulus and Poisson's ratio) the asphaltic concrete creep compliance, and the master creep compliance (using the time-temperature shift function), indirect tensile strength, fracture toughness, the equivalent horizontal load that produces the same stress in the asphalt over the joint as thermal contraction, the pavement geometry (thickness, overlay thickness joint/crack spacing), as well as the coefficient of

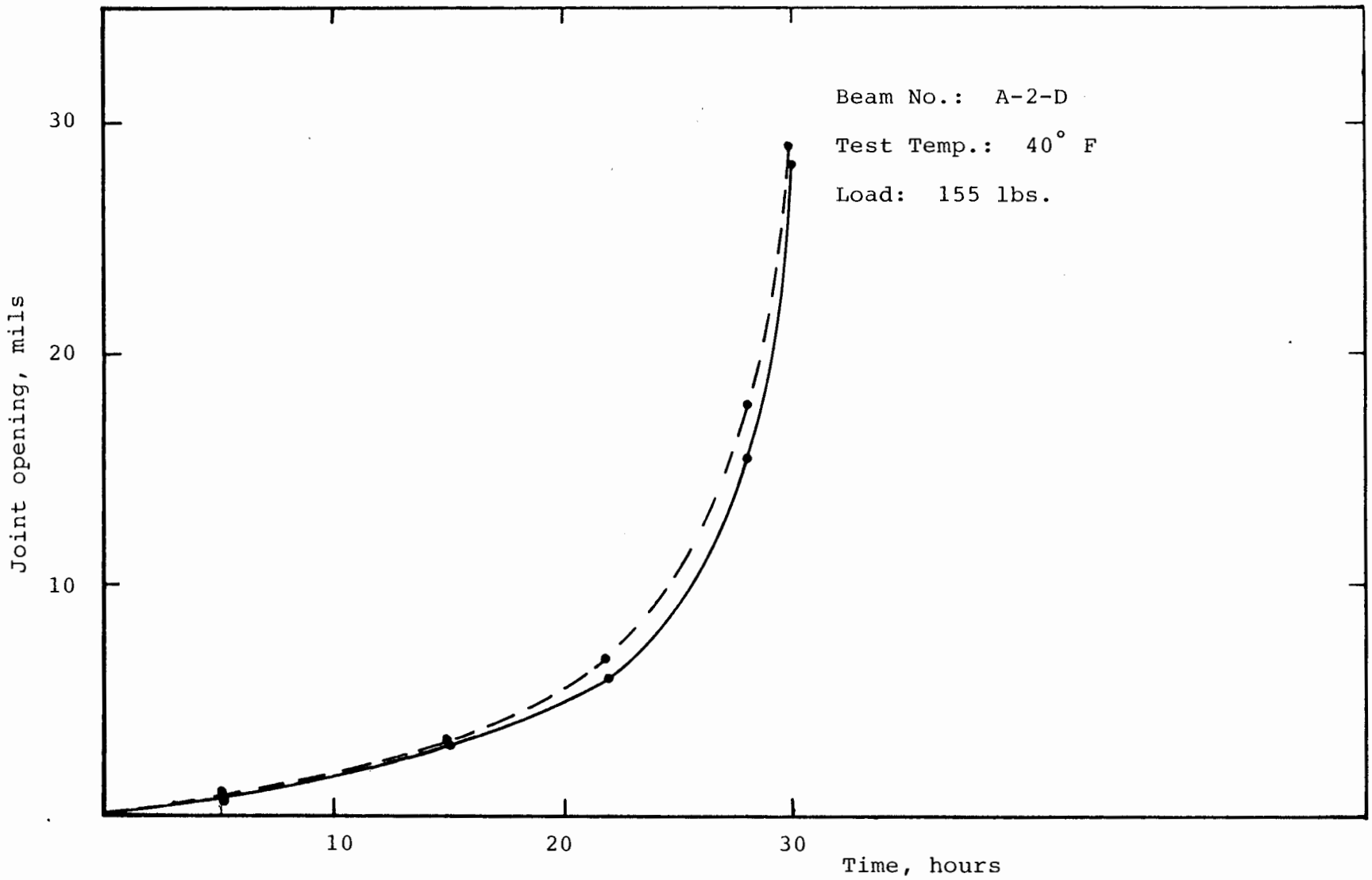

Figure 14 Comparison of Actual and Predicted Joint Opening for Small-Scale Beams.

friction between the concrete slab and the subbase/subgrade. One method of obtaining the friction value is to make the joint movement measurements as a function of slab temperature recommended by the ARE method; however, since the coefficient of friction is most likely variable from location to location, the values presented in table 6 may be used without appreciable loss of accuracy [9]. The fracture toughness can be found through a simple test detailed in reference 7 and the remaining material properties (including creep compliance and the master creep compliance function) can be obtained through tests described in reference 6.

Table 6

Coefficient of friction for various materials.

Subbase Type	Coef. of Friction
Surface treatment	2.2
Lime stabilization	1.8
Asphalt stabilization	1.8
Cement stabilization	1.8
River gravel	1.5
Crushed stone	1.5
Sandstone	1.2
Clay subgrade	1.0
Sandy soil	0.9
Tar paper	1.6
Polyethylene sheet	0.5

CHAPTER IV
FIELD EVALUATION

4.1 Introduction

The use of engineering fabrics in asphalt concrete overlays has developed into a major marketing area for fabric manufacturers. The main intent in the use of fabrics as a reinforcing membrane is to (i) prevent or retard the development of reflection cracking and (ii) act as a barrier in the ingress of water after cracks form in the overlay. Laboratory research findings have demonstrated the effectiveness of certain types of fabric reinforcement in retarding reflection cracking. The research has also indicated that the advantages of using fabric membrane as a reinforcement in overlays are greatest at low temperatures, as the allowable strain values are lower, requiring the fabric membrane to play an important part in the prevention of reflection cracking. Fabric membranes have been used for quite some time in the rehabilitation of airport pavements, but standard procedures have not been used for the monitoring of their performance over a period of time. It was therefore considered necessary as a requirement of this task to prepare a data collection plan for monitoring the performance of fabric membranes in field installation. The plan developed was to be used to obtain actual field information of in-service pavements, with emphasis on collection of subjective performanc data on various maintenance treatments using fabric membranes as an interface layer. As a part of the task it was necesary to visit airport sites to collect and record pavement charateristics data, pavement usage data, environmental factors and performance.

4.2 Site Selection

Airport authorities in the country were contacted requesting information on available performance data of fabrics already incorporated in the construction of overlays during the last 3 to

4 years and to indicate future plans/programs for construction activity using fabrics.

Based on the information obtained, it was decided to visit the international airport sites at Memphis, Albuquerque, LaGuardia, Rochester and Minneapolis. Before visiting the airports for field verification, a data collection plan was formulated (figure 15). A review of the data collection plan indicates that all pertinent information pertaining to pavement history, rehabilitation work performed, methods of non-destructive tests performed, etc. are included to facilitate the collection of visual performance data of the airport pavements.

4.3 Field Evaluation

The field evaluation of the selected airports were conducted between July, 1984 and January, 1986. It was found during these field visits that only the Rochester Airport qualified to be included in this study. It was required that the fabric-reinforced overlay be placed over rigid existing pavements; the overlays where fabrics were used at the other airports were over flexible existing pavements. Details of field evaluation for the Rochester Airport are presented in appendix C.

4.4 Field Validation

Since only one airport project could be found to be used for field validation, a literature search was undertaken to find highway projects that could be used for this purpose. The literature is full of references to reflection cracking studies; however, very few of these studies also contain the data required for a rational analysis of performance, and fewer still have the data described in the previous chapter. A thorough search using the TRIS system yielded a New York study by McCullagh which contained three highway overlay projects (but without fabric) that could be used with the developed model; even this report

DATE:
NAME:

TASK F: REQUIRED AIRFIELD INFORMATION

1. General Information Section: T A R Location: Length = Type: F J CR C

   Width: Maintenance: Age:

2. PCR DATA: Always Start: (N-S, E-W, NE - SW direction)
   (Forms & Manual)

3. Pavement Status: New Overlay

4. Traffic:
   (Types of Design Aircraft) ADT= Load= Wheel Configuration=

5. Climate & Environment: Temperatures - Uniform
   Gradient

6. Structural Layers Information:

   0 Top Layers: H= E= υ= Type:
   0 Base Course: H= E= υ= CBR= Type:
   0 Subbase: H= E= υ= CBR= Type:
   0 Subgrade: E= CBR= Type:
   0 Fabric Type: E= υ= α= G= Brand Name:
   0 # of Fabric Layers =
   Location of Fabric: #1= #2= #3=

   (From bottom of surface layer)
   Fabric dimensions:

7. Support: Shoulder Type Side=

8. Rigid Pav. Slab Length: #1= #2= joint width=
   Slab Width: #1= #2= joint width=

9. Dowels: Diam= E= = Length= Spacings:

Figure 15: Data Collection Plan

10. Tie Bars: Diam= E= υ= Length= spacings:

11. Cracks: Location= Width= υ=

12. Other Information: Void Size: Slab#1= #2=

Dowell Looseness =
Concrete: f'_c = α= %Void=
Base: CBR=
Subbase: CBR=
Subgrade: CBR= GI=
Mean Annual Temperature attached
Other Control Data: Lab: Field:

13. Fabric Type Used - If properties of fabric is known, obtain the details.

14. Fabric Laydown Specification.

15. Crack or joint repair if any.

16. Deflection measurements, if available before and after treatment of joints, overlay work etc.

17. Was fabric placement over cracks and joints or if it was full width?

18. Tack coat used?

19. Period of construction.

20. Overlay thickness and mix design.

21. What is the weather like in winter?

22. Photographs of pre-construction if available.

23. Type of aircraft in use on the runway/taxiway.

24. Any other relevant information.

Figure 15: Data Collection Plan

did not contain the pertinent asphalt concrete (A.C.) properties (modulus, creep compliance, fracture toughness, indirect tensile strength) required by the model [10]. As mentioned before, the airports at Albuquerque, Memphis, Minneapolis, LaGuardia and Rochester were visited in an attempt to collect the required data for field validation. However, only the Rochester airport had concrete pavement sections where a fabric was used under the overlay. Therefore, highway pavements were also used in model verification. An overlay project on I-271 near Cleveland, Ohio was selected to be used, along with the Rochester airport and the New York data. The following assumptions were made in these analyses:

1. The master creep compliance is given by

$$J(t') = .000001[\ .25 + 5(\ t\ 10^{-7.91 + 113T}\ )^{1/3}\ ] \qquad (23)$$

where

t' = transformed time

t = time in seconds

T = temperature, F

which is a modification of Schapery's equation to include the average time-temperature shift factor from reference [6].

2. The indirect tensile strength as a function of temperature, T is given (in psi) by [11]:

$$\sigma_y = 1205\ e^{-.0316T} \qquad (24)$$

3. The fracture toughness KIC is 1200 psi (8.3 MPa). This value represents an average over the temperature range considered.

4. The friction coefficient between the slab and subbase is 0.9 (the results are rather insensitive to variations of this value).

5. The 1983-1984 temperature history from reference 12 is applicable.

6. The temperature drops at a uniform rate from the maximum to the minimum average daily temperature in 6 months.

7. It is assumed that the crack grows only during the time when temperature is decreasing.

4.4.1 Overlays Without Fabric Reinforcement

Table 7 shows the data for the three New York projects. Although the seven assumptions listed above regarding asphalt properties had to be made, it is nevertheless felt that these projects could be used for model validation. They are also included to illustrate the use of the new method.

Table 7
Project data for unreinforced overlays.

PROPERTY	5S	9L	29
Overlay Thickness, in (mm)	2.5 (63.5)	2.5 (63.5)	2.5 (63.5)
Concrete Thickness, in (mm)	8.0(203.2)	8.0(203.2)	8.0(203.2)
Joint/Crack Spacing, ft (m)	45. (13.7)	45. (13.7)	94. (28.7)
Max. Daily Temp. * °F (°C)	76.0(24.4)	81.5(27.5)	80. (26.7)
Min. Daily Temp. * °F (°C)	3.5(-15.8)	-1.5(-18.6)	-6.0(-21.1)

* Average of Daily High and Low Temperatures

The first step in this analysis is to divide the design period (6 months for seasonal temperature change) into some number of intervals and determine the average temperature during the interval - - one month in the following examples. If the temperature is assumed to drop uniformly (assumption 6 above), then the loading time (t in equation 23) per analysis interval is proportional to the average temperature at that interval; i.e.,

$$t = to\ (Th - T)\ (Th - Tl) \qquad (25)$$

where

Th = maximum average daily temperature
Tl = minimum average daily temperature
T = current temperature
to = time (in seconds) for temperature to drop from Th to Tl (6 months)

The next step is to determine the creep compliance and the creep modulus (inverse of compliance) and use these values with the EFRON program to compute the joint opening and critical stress (in the asphalt layer above the joint) as a result of the temperature drop.

The EFRON program is also used to determine the equivalent horizontal load (pull) required to generate the same critical stress above the joint as was found in the previous step. This can be done by assuming a load, calculating the resultant stress and taking the ratio of stresses (from this step and previous step). Rigorously, an iterative process should be used since iteration is required whenever the shear stress exceeds the maximum shear (at the slab-subbase interface); however, this effect is negligible for all practical purposes.

The results of EFRON analysis are shown in tables 8 through 11. The projects 5S, 9L and 29 are actual projects from

Table 8
Analysis for project 5S.

Time Mo.	Avg. Temp. °F	°C	Avg. Modulus ksi	(MPa)	Joint Opng in	(mm)	Load lb	(N)	% Joints Cracked
0	76.0	(24.4)	2.15	(14.8)	0	0	0	(0)	0
1	70.0	(21.1)	2.20	(15.2)	.0371	(0.942)	198	(880)	--
2	57.9	(14.4)	3.60	(24.8)	.0734	(1.864)	255	(1134)	64.0
3	45.8	(7.7)	9.00	(62.1)	.1066	(2.708)	454	(2019)	72.0
4	33.8	(1.0)	23.0	(159.)	.1339	(3.401)	841	(3741)	96.0
5	21.7	(-5.7)	58.0	(400.)	.1526	(3.876)	1396	(6209)	96.0
6	9.5	(-12.5)	153.	(1055)	.1628	(4.135)	1975	(8788)	96.0

Table 9
Analysis for project 9L.

Time Mo.	Avg. Temp °F	°C	Avg. Modulus ksi	(MPa)	Joint Opng in	(mm)	Load lb	(N)	% Joints Cracked
0	81.5	(27.5)	0.94	(6.48)	0	0	0	(0)	0
1	74.6	(23.7)	1.26	(8.69)	.0432	(1.097)	182	(810)	-
2	60.7	(15.9)	2.85	(19.6)	.0858	(2.179)	257	(1143)	23.1
3	46.9	(8.3)	7.85	(54.1)	.1240	(3.150)	474	(2108)	61.5
4	33.1	(0.6)	23.5	(162.)	.1550	(3.937)	976	(4341)	42.3
5	19.2	(-7.1)	70.0	(483.)	.1774	(4.506)	1736	(7722)	80.3
6	5.4	(-14.8)	200	(1379)	.1838	(4.669)	2414	(10737)	88.5

Table 10

EFRON analysis for project 29.

Time Mo.	Avg. Temp. °F	°C	Avg. Modulus ksi	(MPa)	Joint Opng in	(mm)	Load lb	(N)	% Joints Cracked
0	80.0	(26.7)	1.15	(7.92)	0	0	0	0	0
1	72.8	(22.7)	1.50	(10.3)	.0878	(2.230)	693	(3082)	-
2	58.5	(14.7)	3.40	(23.4)	.1700	(4.318)	863	(3839)	-
3	44.2	(6.8)	10.1	(69.6)	.2374	(6.030)	1326	(5898)	72.5
4	29.9	(-1.2)	30.9	(213.)	.2805	(7.1225)	2082	(9261)	74.5
5	15.5	(-9.2)	100.	(689.)	.3000	(7.620)	2829	(12583)	98.0
6	1.2	(-17.1)	290.	(1999)	.3077	(7.816)	3240	(14412)	98.0

Table 11

EFRON analysis for project 29a.

Time Mo.	Avg. Temp °F	°C	Avg. Modulus ksi	(MPa)	Joint Opng in	(mm)	Load lb	(N)	% Joints Cracked
0	80.0	(26.7)	1.15	(7.92)	0	0	0	0	NA
1	72.8	(22.7)	1.50	(10.3)	.0446	(1.133)	195	(885)	NA
2	58.5	(14.7)	3.40	(23.4)	.0878	(2.230)	293	(1303)	NA
3	44.2	(6.8)	10.1	(69.6)	.1265	(3.213)	573	(2549)	NA
4	29.9	(-1.2)	30.9	(213.)	.1559	(3.960)	1192	(5302)	NA
5	15.5	(-9.2)	100.	(689.)	.1720	(4.369)	2060	(9163)	NA
6	1.2	(-17.1)	290.	(1999)	.1792	(4.552)	2660	(11832)	NA

NA - Not applicable.

reference 10, and project 29a is the same as 29 except that the joint spacing has been reduced to 45 feet (13.7 m) to illustrate the effect of joint spacing. Also shown in tables 8 through 10 is the history of reflection cracking development (under the column heading % of joints cracked).

The results of the EFRON analysis (joint opening and load) are input into RECK along with temperatures, indirect tensile strength, fracture toughness, and the geometry of the pavement. The output of the RECK program is the predicted time (in hours) for the reflection crack to grow to 90% of the way through the overlay. The 90% value, rather than 100% is used because the stress intensity factor becomes unbounded at the surface and, in any case, the crack growth rate beyond 90% is very rapid.

It should be noted that because of assumption 7 above, if the time to failure is less than 4320 hours, the failure time in months is obtained simply by dividing the time by 720; however, if the failure time is between 4320 and 8640 hours, the time in months is 6 + time/720, and if the time is between 8640 and 12960 hours, the time in months is 12 + time/720, etc.

Table 12 shows the predicted time, in months, for failure, and the corresponding percentage of reflection cracking that actually occurred. While the agreement between predicted and actual failure times are not perfect, the predicted times are reasonably consistant with observed cracking. Also, the comparison of results for projects 29 and 29a indicate that shortening joint spacing decreases the amount of joint opening and increases the time to failure, as is expected.

A comparison of projects 5S, 9L and 29a show the effect of temperature, although since both maximum and minimum temperatures change for these projects, the temperature effect is somewhat more difficult to isolate. However, comparison of 9L and 29a (where the temperature drop is nearly the same) shows that lower

Table 12
Predicted failure times.

	5S	9L	29	29a
Jnt. Opening in (mm)	.163(4.14)	.285(4.67)	.308(7.82)	.179(4.5)
Predicted Times Hrs.	8986	4830	1622	4120
Predicted Time Mo.	24.5	12.7	2.3	5.7
% Cracking at Time	100	100	<72.5	NA
Time at 100% Crack	15	7	8	NA

NA - Not Applicable

to failure; i.e., reflection cracking is more severe in colder climates.

4.4.2 Overlays with Fabric Reinforcement

Fabric reinforcement of overlays of rigid pavements was used on selected joints of I-271 in Cleveland, Ohio, and on sections of the main (rigid) runway at the Rochester International Airport. The pertinent data for these projects is shown in table 13.

The same analysis procedure that was discussed in the previous section was again used. The results of EFRON analysis are presented in tables 14 and 15 for I-271 and Rochester airport, respectively. These were input into the RECK program to obtain the predicted failure times. The program predicts that reflection cracking should occur in the I-271 pavement in 15.3 months (approximately 1.5 winters) and in the Rochester runway pavement in approximately 75 years; i.e., thermally induced reflection cracking will not be a problem at Rochester. It needs to be emphasized that it is assumed in the reflection cracking

Table 13
Project data for fabric reinforced overlays.

Property	I-271	Rochester
Overlay thickness, in (mm)	3.0 (76.2)	6.0 (152.4)
Concrete thickness, in (mm)	10.0 (254.0)	11.0 (279.4)
Joint/crack spacing, ft (m)	60 (18.3)	25 (7.6)
Max. daily temp. * ^{o}F (^{o}C)	80.5 (26.9)	80.0 (26.7)
Min. daily temp. * ^{o}F (^{o}C)	-11.5 (-24.2)	3.0 (-16.1)
Fabric Type	Petromat	Petromat
Fabric Effectiveness	3.05	3.05

*Average of daily high and low temperatures.

analysis that no other distresses occur and that the seasonal temperature cycles are the only cause of reflection cracking formation. In reality many other factors are present so that the pavement is not expected to last 75 years.

The overlay on I-271 was placed during May, 1984 and the performance rated during December, 1985 and again during March, 1986. It was found during the December, 1985 rating that approximately 85 percent of the joints had reflected through the overlay; the March, 1986 rating showed this value to be nearly 100 percent. Thus, the predicted time of 15.3 months agrees very well with the observed value of between 19 and 22 months (1.5 to 2 winters). The predicted time for reflection cracking to occur in an unreinforced overlay is 3.0 months (0.5 winters). This analysis indicates that the 2.5 in (63.5mm) overlay is too thin for fabrics to be of any significant benefit. The overlay thickness for the prevention of thermally induced reflection cracking could be determined using this analysis method.

Table 14

EFRON analysis of I-271

Time Mo.	Avg. Temp. °F	°C	Avg. Modulus psi	(MPa)	Joint Opng in	(mm)	Load lb	(N)	% Joints Cracked
0	80.5	(26.9)	0.27	(1.86)	0	0	0	0	0
1	72.8	(22.7)	0.56	(3.86)	.0601	(1.526)	268	(1192)	-
2	57.5	(14.2)	2.12	(14.6)	0.1228	(3.120)	368	(1637)	-
3	42.2	(5.7)	7.95	(54.8)	.1802	(4.577)	701	(3118)	-
4	26.8	(-2.9)	30.0	(207.)	.2233	(5.673)	1571	(6988)	-
5	11.5	(-11.4)	112.	(772.)	.2457	(6.242)	2864	(12739)	-
6	-3.8	(-19.9)	390.	(2689)	.2541	(6.454)	3809	(16943)	-

Table 15

EFRON analysis of Rochester International Airport.

Time Mo.	Avg. Temp °F	°C	Avg. Modulus psi	(MPa)	Joint Opng in	(mm)	Load lb	(N)	% Joints Cracked
0	80.0	(26.7)	0.70	(4.83)	0	0	0	0	0
1	73.6	(23.1)	1.21	(8.34)	.0228	(0.580)	64	(283)	-
2	60.8	(16.0)	3.75	(25.9)	.0452	(1.148)	126	(560)	-
3	47.9	(8.8)	11.5	(79.3)	.0664	(1.687)	304	(1350)	-
4	35.1	(1.7)	35.6	(245.)	.0845	(2.148)	756	(3360)	-
5	22.3	(-5.4)	105.	(721.)	.0974	(2.474)	1564	(6949)	-
6	9.4	(-12.6)	295.	(2034)	.1044	(2.652)	2517	(11186)	-

The fabric-reinforced overlay at the Rochester International Airport had been in service through about two winters at the time of rating. A detailed inspection of the main runway where fabric was used showed that not a single joint had reflected through. Although this observation does not validate the 75 year prediction, it certainly is encouraging. Monitoring of the performance of this pavement over the next several years is needed to further verify the prediction model. The monitoring should be conducted in areas of low traffic to isolate thermally induced cracking from fatigue effects.

4.4.3 Summary of Field Evaluation

As discussed in the previous section, the newly developed thermally induced reflection cracking prediction model was applied to four highway and one airport pavement overlay project. The model predicted the time for reflection cracking to occur to within a few months of when 100 percent reflection cracking actually took place for the four highway projects. This agreement is excellent, especially in view of the fact that certain assumptions (listed in section 4.4) had to be made about the overlay properties.

The model also predicted that thermally induced reflection cracking would not develop in the overlay at Rochester Airport - the predicted time is 75 years. This overlay was built during the 1984 construction season and has been in service through two winters; at the last rating not a single joint had reflected through this overlay. While survival through two winters does not necessarily validate the 75 year prediction, it strongly suggests that reflection cracking is not expected to be a problem with this overlay. Thus, all five field validation projects are in strong accord with the prediction model.

CHAPTER V

SPECIFICATIONS FOR MATERIAL PROPERTIES, TESTING PROCEDURES, AND CONSTRUCTION METHODS

5.1 Introduction

Specifications for fabrics used to reinforce asphalt overlays have been predominantly those suggested by fabric manufacturers and adopted by the States to local use. Physical property requirements have focused on weight, tensile strength, and elongation. The tests conducted on fabrics used in pavement reinforcement are the same as those used in textile testing generally and do not always provide the parameters necessary for engineering analysis.

Presently, States' specifications either include the recommendations of the manufacturer or contain some modification of manufacturers's specifications. Data have not been furnished to date that would confirm the need for, or the significance of, values obtained for certain tests. Certainly the pavement overlay environment involves stresses and strains that are probably not applicable to erosion, drainage, or separation.

Texas specification values for fabrics in overlays are based on field and laboratory studies and appear to come the closest to correlating fabric properties to overlay requirements [12]. Nonetheless, there remains a gap between what is specified and what is actually required to provide a cost effective and durable overlay system. The factors affecting long term satisfactory performance of an overlay are complex when taken as an interacting system. Those factors include: weight and thickness of the overlay; overlay lay-down temperature and compaction; type of overlay mix design; ambient temperature at the time of fabric and/or asphaltic concrete placement; type of tack coat and its rate of application; condition of the existing pavement; anticipated traffic loading; and anticipated distribution of

stresses and strains at and adjacent to cracks in the underlying pavement. Only recently have efforts been made to determine the reinforcement requirements that would relate to the physical properties of fabrics.

At present, the Texas and California specifications for overlay fabrics are those that permit competition among fabric manufacurers while assuring a higher quality fabric system. The Texas specification adds the dimension of asphalt retention although the minimum value of 0.5 ounces/square-foot (304 gm/sq. m) is significantly lower than that of the Phillips Fibers Corporation which recommends a minimum of 0.20 gallons/square yard (2.8 ounces/square foot (1702 gm/sq. m)). Georgia also has a minimum asphalt retention value requirement utilizing a Georgia test procedure.

The properties of a fabric membrane proposed for use in the prevention of reflection cracking in asphalt overlays are described in this chapter. The specifications as prepared by Texas Department of Highways are detailed below, after certain modifications for airfield pavements [13]. The fabric underseal shall consist of a single application of asphalt tack coat covered with a layer of fabric membrane with or without sand or screening [13].

5.2 Materials

The non-woven fabric shall be made of thermoplastic fibers. These fibers in the fabric membrane shall be oriented in either aligned or random orientation and the fibres may be either continous or discontinous throughout the fabric. The fabric membrane itself shall be rot proof and shall be compatible for use with asphalt cements.

5.2.1 Physical Properties

The fabric membrane shall meet the requirements listed in table 16 when sampled and tested according to ASTM test procedures.

5.2.2 Packaging Requirements

The fabrics shall be packed in standard width rolls of specified length. The fabrics shall be uniformly wound onto suitable cylindrical forms to aid in handling and unrolling. The packing of the fabric shall be such that it is not damaged due to ultra-violet light and moisture during normal storage and handling.

5.2.3 Identification Requirements

Each roll shall be identified by the manufacturer as to lot number or control numbers, date of manufacture, total weight, width and length of fabric and gross weight.

5.2.4 Sampling Requirements

Individual samples shall be cut from at least one roll selected on a random basis from each of 50 rolls or fraction thereof representing each shipment.

5.2.5 Acceptance Criteria

Individual rolls shall meet the weight requirement; any deviation shall result in rejection of that roll. Should any individual sample fail to meet any specification requirement, then that roll shall be rejected and two additional samples shall be taken, one from each of two other additional rolls selected at random from the same 50-roll lot. If either of these two samples fails to meet the specification requirement, then the whole consignment of 50-rolls shall be rejected.

Table 16
Requirements for fabrics.

TEST Original Physical Properties	METHOD	REQUIREMENT Minimum	Maximum
Fabric weight, oz./sq.yd.	ASTM D 1910 paragraph 37 or 38	4.0	9.0
"Apparent elongation" at "breaking load" on warp-wise specimens, percent.	ASTM D 1682, Grab Method G as modified by paragraph F. Testing Requirements of this specification.	50	150
"Apparent elongation at "breaking load" on filling-wise specimens, percent.	" " "	50	150
"Breaking load," on warp-wise specimens, pounds	ASTM D 1682, Grab Method G as modified by paragraph F. Testing Requirements of this specification.	45	---
"Breaking load," on filling-wise specimens, pounds.	" " "	80	---
Asphalt retention, oz./sq.ft.	Section 5.2.6 Testing Requirements on this specification.	0.5	8.5
Change in area caused by asphalt retention test and subsequent asphalt removal. Reported as change in area of specimen measured after test as compared to area of specimen prior to test, percent.	Section 5.2.6 Testing Requirements of this specification.	--	± 15

5.2.6 Testing Requirements

The tests described below are intended to assure a uniform product meeting certain minimum requirements. These tests have been used successfully by various State departments of transportation and would fit in with the work performed by Resource International, Inc. (RII) but are not directly justified by the research. The tests fit in with the RII research because the fabrics used all meet the tests described below.

Fabric weight determinations may be made upon complete rolls of fabric. In addition, the individual test samples, selected in accordance with the sampling procedure outlined, may be used for fabric weight determination. If individual test samples are used for fabric weight determination, then all 4 x 8 inch (102 x 203 mm) specimens required for testing of a roll shall be selected from the one-foot (0.3 m) roll-width test sample, the individual test specimens shall be weighed and the average weight expressed in ounces per square yard (gms per sq. meter), and calculated and reported on that basis.

The determination of the "breaking load" and the "apparent elongation" at "breaking load" shall be made in accordance with ASTM D 1682, entitled "Standard Methods of Test for Breaking and Elongation of Textile Fabrics," using Grab Method G with a constant rate of traverse so that the breaking load is reached in 20 seconds plus or minus three seconds. Modified jaws are to be used in which the 1 x 2 inch (25 x 51 mm) jaw faces are serrated with approximately 0.5 millimeter deep serrations in a horizontal direction when the jaws are pulled vertically. The continuous teeth or serrations are to be pointed slightly upward on the jaw faces as the jaws are positioned in the testing machine. Original Physical Property test specimens, as placed in the testing machine, shall be rectangular and measure four by eight

inches (102 x 203 mm). When placed in the 1 x 2 inch (25 x 51 mm) modified jaws, the fabric shall extend 1/2 inch (12 mm) on either side of the one-inch wide by two inch (25 x 51 mm) high jaws.

Five individual specimens shall be chosen for determination of original physical properties (tensile and elongation testing) in the warp-wise direction and eight individual specimens shall be chosen for testing in the filling-wise direction. It is important that these specimens be chosen at random from each individual test sample of at least one foot (0.3 m) in length by full roll width, selected at random in accordance with the prescribed sampling procedure. The average test value obtained on the five specimens and the average test value for the eight specimens tested shall be reported as the final test values for those tests in the warp and fill directions, respectively. Additional individual specimens shall be selected for those tests involving hot asphalt.

Asphalt retention and potential change of area of the fabric shall be determined as follows:

Three warp-wise specimens of four by eight inches (102 by 203 mm) and three filling-wise specimens of like dimension shall be selected at random from the individual one foot (0.3 m) wide by full width sample. These tests specimens shall be individually weighed to the nearest 0.1 gram and then submerged for 30 minutes in the specified asphalt cement maintained at a temperature of 275 ± 4 degrees F (135 ± 2 degrees C) in a mechanical convection oven. After the required submersion the test specimens shall be removed and hung to drain in the oven for an additional 30 minutes at 275 ± 4 degrees F (135 ± 2 degrees C). The samples shall then be removed from the oven and allowed to drain for one hour at a temperature of 76 ± 4 degrees F (24 ± 2 degrees C).

After the drain period of one hour the specimens shall be weighed to the nearest 0.1 gram and then placed in naptha heated to 110 ± 5 degrees F (43 ± 2 degrees C) for 30 minutes. After all the asphalt has been removed from the sample, the specimens will be blotted and allowed to air dry. The area of the specimen shall then be measured for determination of percentage change in area. Asphalt retention and change in area shall be calculated.

Load test specimens which have been previously subjected to the 275 degrees F (135 degrees C) Asphalt Retention Test and Asphalt Removal procedures shall be centered in the jaws of the tensile testing machine. Three inch (76 mm) jaw separation shall be maintained. If the original 4 x 8 inch (102 x 203 mm) specimen has expanded or shrunk in size, it may not be possible to maintain the required fabric spacing around the jaws. Specimens will be centered and 3 inch (76 mm) jaw separation maintained.

5.3 Construction Methods

The area on which the tack coat and fabric is to be placed shall be clean of dirt, dust or other deleterious material by sweeping or other approved methods. Asphaltic materials of the type and grade shown on the plans shall be applied on the clean surface by an approved type of self-propelled pressure distributor so operated as to distribute the material in the quantity specified, evenly and smoothly under a pressure necessary for proper distribution. Also provide all necessary facilities for determining the temperature of the asphaltic material for determining the rate at which it is applied and for securing uniformity at the junction of two distributor loads. The distributor shall have been recently calibrated and the engineer shall be furnished an accurate and satisfactory record of such calibration.

The tack coat shall not be applied when the air temperature is below 60 degrees F (15 degrees C) and is falling, but it may

be applied when the air temperature is above 50 degress F (10 degrees C) and is rising; the air temperature being taken in the shade away from artificial heat. Neither the asphalt nor the fabric shall be placed when general weather conditions, in the opinion of the engineer, are not suitable.

After beginning the work, should the yield (distribution rate) on the asphaltic material appear to be in error, the distributor shall be calibrated in a manner satisfactory to the engineer before proceeding with the work. It was concluded in Volume I that tack coat quantity is an important variable; therefore careful attention should be paid to tack coat application rates [1].

Asphaltic material shall be applied ahead of the placement of the fabric in widths 10 inches (254 mm) wider than the fabric. The asphaltic material shall be applied at the approximate rate shown on the plans or as directed by the engineer.

Immediately upon application of the asphalt, the fabric shall be aligned and carefully broomed and/or rolled into the asphalt with equipment approved by the engineer. In the event the initial alignment is not satisfactory and causes the fabric to wrinkle during placement, the fabric shall be cut and realigned, overlapping the previous material, and proceeding as before. All transverse joints shall be overlapped a minimum of 6 inches (152 mm). In lapping joints, the top fabric shall be folded back to allow application of a light coat of asphalt. The top fabric is then folded back onto the asphalt and broomed and squeegeed out smoothly. Rolling and /or brooming the fabric into the asphalt at the joints shall be accomplished in such a way that the air bubbles which form under the fabric will be removed. This may be accomplished by brooming from the center of the fabric toward the outer edges. The fabric shall be neatly cut and contoured at all joints as directed.

If the edges of the fabric tend to be displaced because of air currents, the edges shall be secured to the pavement at 15-foot (4.6 m) intervals. In the event this procedure does not prove satisfactory, then work will be suspended until conditions are more favorable.

Adjacent panels of the fabric shall overlap a minimum of 4 inches (102 mm). Additional asphalt shall be applied to make these longitudinal joints.

Turning of equipment shall be gradual and kept to a minimum to avoid damage to the fabric. On typical sections not receiving a seal coat, the surface of the fabric shall be covered with a thin layer of clean sand or clean crusher screenings at a rate sufficient to absorb the excess asphalt. The sand and/or crusher screenings shall be approved by the engineer. On typical sections to be seal coated, only sufficient sand shall be spread ahead of the tires to prevent sticking.

All storage tanks, piping, retorts, booster tanks and distributors used in storing or handling asphalt material shall be kept clean and in good operating condition at all times, and they shall be operated in such a manner that there will be no contamination of the asphaltic material with foreign material. It shall be the responsibility of the contractor to provide and maintain, in good working order, a recoding thermometer in the storage heating unit at all times.

The engineer will select a temperature of application based on the temperature viscosity relationship that will permit application of the asphalt within the limits recommended for "Asphalts, Oils and Emulsions". The recommended range for the viscosity of the asphalt is 50 seconds to 60 seconds Saybolt Furol.

The A.C. overlay may be placed as soon as the fabric is in place provided that the surface is dry and the weather conditions

are such that proper handling, finishing and compaction can be accomplished. The air temperature shall be greater than the minimum values given below [14].

Course Thickness	Minimum Air Temperature
3 in (76 mm) and over	35 ^{o}F (2 ^{o}C)
1.5 to 3 in (38 to 76 mm)	40 ^{o}F (4 ^{o}C)
1 to 1.5 in (25 to 38 mm)	50 ^{o}F (10 ^{o}C)*
less than 1 in (25 mm)	50 ^{o}F (10 ^{o}C)

* 40 ^{o}F (4 ^{o}C) may be used if pneumatic tire roller is added to the roller train.

Some highway agencies recommend that the fabric treated surface be opened to traffic for 24 hours prior to placement of the overlay (in order to achieve better adhesion) provided that the traffic forces do not tear the fabric [14]. This, however, is not considered a good practice for airport work, particularly in touchdown and takeoff areas and areas where aircraft turning is taking place.

CHAPTER VI
CONCLUSIONS AND RECOMMENDATIONS

6.1 Conclusions

6.1.1 RECK Model

A new model was developed in this study to analyze the phenomenon of thermally induced reflection cracking of asphaltic concrete overlays over portland cement concrete pavements. This model is based on fundamental material properties (creep compliance, fracture toughness, indirect tensile strength) and does not depend on any empirical distress functions. When applied to fabric-reinforced overlays, however, a fabric effectiveness factor is required. This factor is obtained from simple laboratory tests on beams being pulled apart by a constant force simulating stresses due to thermal contraction, and represents the ratio of failure times of reinforced and unreinforced (control) beams, as described in section 3.3.

The developed model has been validated by application to both laboratory specimens and field pavements. Two types of laboratory tests were used: (1) small-scale beams (3 x 3 x 24 in (76 x 76 x 610 mm)) being pulled apart by a constant force, and (2) large-scale beams (8 x 12 x 96 in (203 x 305 x 2438 mm)) being pulled apart at a constant strain rate. The model was equally successful in predicting failure times for both sets of tests, as indicated in the figures presented in appendix B. Other than the size factor, the small-scale and large-scale beam tests are quite different - in one case there is constant load and a variable strain rate (small beams) whereas in the other case a constant strain rate is applied and a variable load (stress) results. Success in the prediction of failure times for both sets of tests has to be regarded as a more significant validation than if only one type of test had been performed.

The application of the new theory to field pavements was discussed in chapter IV. It was shown that the model predicted the formation of thermally induced reflection cracks to within a few months of their actual occurrence on four out of five projects. The models also predicted that the fifth project would not experience reflection cracking for a considerable time (75 years) - after two winters and almost two years in service, not a single reflection crack has appeared. Although several assumptions had to be made in the analysis of field pavements, the close agreement with field performance is a strong indicator of the model validity, especially when considering the success in predicting failure times for the laboratory tests.

The reflection cracking analysis model has been computer coded in a program called RECK. The program listing and user manual are presented in appendix A. Only the RECK program is required for the analysis of laboratory beams, but application to field pavements requires that the EFRON program be used first to develop some of the inputs required by RECK, as discussed in chapter IV. The EFRON program was developed during phase I of this study and appears in Volume I of this report [1].

It should be emphasized that the reflection cracking model developed in this study represents a significant advance in the analysis of the reflection cracking phenomenon, not only because the dependence on empirically developed distress functions has been eliminated, but also because the model considers the asphaltic concrete as a viscoelastic material. While asphaltic concrete can be considered as an elastic material under dynamic (short duration) loading due to aircraft, thermally induced stresses develop over about six months period, requiring viscoelastic analysis.

6.1.2 Use of Fabrics for Cracking Retardation

It has been shown in this study (including phase I of this project) that the use of non-woven fabrics as reinforcing of

flexible overlays over rigid pavements can be beneficial in retarding the development of both fatigue (load associated) and reflection (thermally induced) cracking. The fabric reinforcement has been quite effective in increasing fatigue life of laboratory specimens due to dynamic loading, particulary at lower temperatures where fabric effectiveness factors of 3 to 10 have been noted. The laboratory studies also indicate that the use of fabrics can be beneficial in extending the time at which thermally induced reflection cracking occurs. Fabric effectiveness factors of around 2 to 3 have been obtained. It should, however, be pointed out that the above studies are not intended to be a blanket endorsement of the use of fabrics with flexible overlays of rigid pavements. The tests and conclusions discussed in this report are applicable to two mechanisms of cracking: (1) fatigue due to dynamic loading, and (2) thermal stresses due to seasonal temperature changes. The model does not address thermal fatigue (daily temperature cycles), nor does it consider the shear stresses developed over joints and cracks that have poor load transfer ratios and high differential deflections. The judgement of the engineer, particularly in regard to load transfer and differential deflection across joints and cracks, is invaluable when deciding on the use of fabric reinforcement.

6.2 Recommendations on the Use of Fabrics

Based on the research carried out in this study, the following recommendations are offered regarding the use of fabric reinforcement:

1. For runway/taxiway rehabilitation projects which include pavement widening with new asphaltic concrete overlays, fabrics placed longitudinally over the shoulder-pavement and/or widening joint should be considered. An impermeable fabric system is perferred.

2. Rather than placing the fabric on the cracked existing runway/taxiway, construct an asphalt leveling course

first so as to provide a relatively unblemished surface for applying the tack coat and the fabric.

3. Prior to placement of a fabric overlay system the condition of the existing runway/taxiway should be documented. When an unstable (poor load transfer and partial support at joints) runway/taxiway is suspected, deflection tests are recommended. While limiting deflection values have yet to be established for fabric systems, it is important that data be obtained that could assist in their eventual evaluation.

4. Over concrete runway/taxiway, use of heavy duty fabric systems in strips over transverse and pavement edge joints and cracks is recommended. However, joints with poor load transfer or partial support should be restored first.

5. Since all fabrics are not equivalent in physical properties, agencies should conduct tests detailed in chapter V, including the asphalt retention tests so as to develop documentation that may be useful later in assessing relative fabric performance.

6.3 Recommendations for Future Research

The model developed in this study to predict the formation of thermally induced reflection cracking appears to be very successful when applied to flexible overlays of rigid pavements. It is however, not applicable to the analysis of overlays over flexible pavements where thermally induced movements may be significant (i.e., for flexible pavements with low temperature cracking) because a model to predict thermal movements of viscoelastic pavements is needed. The EFRON program is able to predict these movements in an elastic pavement (including a viscoelastic overlay) but needs to be modified to include the

effect of subgrade friction on a viscoelastic slab. The RECK program can then be used (with the inputs from a modified EFRON analysis) to predict thermally induced reflective cracking in asphaltic concrete overlays of both rigid and flexible pavements.

Fabric effectiveness factors have been developed for a few non-woven fabrics (including the fiber SAMI layer); similar data is needed for woven fabrics. This requires laboratory testing of beams under fatigue and simulated thermal loading conditions. The testing procedures developed for use in this study are recommended to be used.

REFERENCES

1. Majidzadeh, K., Ilves, G.J., Sklyut, H., and Kumar, V.R., "Mechanistic Methodology for Airport Pavement Design with Engineering Fabrics, Volume I: Theoretical and Experimental Bases," DOT/FAA/PM-84/9,I, August, 1984.

2. Majidzadeh, K., et al, "Application of Fracture Mechanics for Improved Design of Bituminous Concrete," Final Report, FHWA-RD-76-91, U.S. DOT, Federal Highway Administration, June 1976.

3. Schapery, R.A., "A Theory of Crack Initiation and Growth in Viscoelastic Media, I. Theoretical Development," International Journal of Fracture, Volume II, No. 1, February, 1975.

4. Grahma, G.A.C., "The Correspondence Principle of Linear Time-Dependent Boundary Regions," Quarterly of Applied Mechanics, Vol. 26, 1968, pp. 167-174.

5. Dugdale, D.S., "Yielding of Steel Sheets Containing Slits," Journal of the Mechanics and Physics of Corresp. Principle."

6. Kenis W.J. "Predictive Design Procedures, VESYS User's Manual," FHWA-RD-154, January 1978.

7. Karakouzian, M., "A Simplified Method for Material Testing and Design of Pavement Systems." Ph.D. Dissertation, The Ohio State University, Columbus, 1978.

8. Majidzadeh, K., and Ilves, G.J., "Improved Methods to Eliminate Reflection Cracking" Final Report of Project DTFH-61-C-0120, June, 1985.

9. Treybig, H.J., et al, "Overlay Design and Reflection Cracking Analysis for Rigid Pavements - Volume 1," Final Report FHWA-RD-77-66, U.S. DOT, Federal Highway Administration, August, 1977.

10. McCullagh, F.R., "Reflection Cracking of Bituminous Overlay of Rigid Pavements," Special Report 16, Engineering Research and Development Bureau, New York State Department of Transportation, State Campus, Albany, New York, February 1973.

11. Karaki, A., "Engineering Characteristics of Hot-Recycling Asphalt Materials," MS Thesis, The Ohio State University.

12. "Climatological Data Annual Summary," New York, 1983, Volume 88 Number 13, NOAA ISSN 0364-6041.

13. Special specifications for fabrics - Texas Department of Highways.

14. "Construction and Material Specifications," State of Ohio Department of Transportation, 1986.

APPENDIX A
THE RECK PROGRAM

A.1 USERS MANUAL

A.1.1 Introduction

This computer program is designed to analyze reflective cracking of flexible overlays over rigid pavements above underlying cracks or joints due to thermal loading only (loads induced by the horizontal temperature movement and vertical curling and warping of the slabs) after the construction of the overlays.

This program is based on the analysis of the facture mechanics of a viscoelastic material by Schapery and others [3].

Schapery's work has been adopted, with some modification, to develop the mathematical formulations of the present model described in chapter 3. The reason behind using such an approach emerges from the fact that engineering materials, especially the asphaltic mixture and fabrics, exhibit time dependent behavior and hence the crack initiation and propagation are time dependent events.

A.1.2 Input and Output for the Developed Model

The developed model requires easy to find input parameters that could be obtained from laboratory tests. Parts of these parameters are the properties of the overlay material such as the creep compliance, J(t), the fracture strength, σ_y, and the fracture toughness, K . The other part of the input data are the load-crack opening displacement values. For a laboratory test, the induced thermal loadings are simulated by applying a variable horizontal pull and measuring the joint opening. For a field case, the joint opening can be calculated over a specific period of time knowing the temperature variation within that time. Also, an equivalent horizontal load can be calculated to

simulate the induced thermal stresses. The joint opening and load calculations can be performed using the computer program EFRON [1].

Using the previous input data, the program predicts the time at which failure occurs. Also a part of the output is the crack lengths at different time intervals.

A.1.3 Description of Input Data

Table 17 shows a description of the input data.

The equation used for creep compliance J(t) is:

$$J(t,T) = C1 + C2(t \times 10^{C3})^{m}$$

where:

C1, C2 and m are constants; the program uses the following default values if non-zero values for these constants are not input.

C1 = 0.3935 x 10 C2 = 0.787 x 10 m = 0.345
C3 is a function of temperature and is given by:
C3 = -5.019 + 0.07171 T.

The fracture strength of the overlay material is given by:

$$\sigma_y = 1205\ e^{-0.0316\ T}$$

Table 17

Description of input data.

CARD	FORMAT	VARIABLE	COL.	DESCRIPTION AND VALUE RANGE	COMMENTS
1	3I5	ICASE	1-5	Case Option: = 1 - 'Laboratory Test' = 2 - 'Field Case'	
		IOPN	6-10	Beam Option: = 1 - 'Small Scale Laboratory Beam' = 2 - 'Large Scale Laboratory Beam' = Ø - 'Field Case'	
		NB	11-15	Beam or Field Case Number	
2	I15	NUMNP	1-5	Number of Time Stations at which Joint Openings are Measured.	
3	3D15.6	TH1	1-15	Overlay Thickness	For a Field Case take WID = 1.00
		TH2	16-30	Concrete Base Thickness	
		WID	31-45	Beam Width (for Laboratory Case)	
4	3D15.6	CONI	1-15	Value of C_1 in the Creep Compliance Equation. (Default value = 0.080×10^{-6}) Value of C_2 in the Creep Compliance Equation (Default Value = 0.7920×10^{-5}) Value of m in the Creep Compliance Equation (Default value = 0.345).	For Default values, Leave Card No. 4 Blank

Table 17 (continued)

CARD	FORMAT	VARIABLE	COL.	DESCRIPTION & VALUE RANGE	COMMENTS
5	1D15.6	RKC	1-15	The Fracture Toughness of the Overlay Material	
6 N	5D15.6	PT(I)	1-15	Time at which Joint Opening and load are measured.	N = 5+NUMNP I = 1,2,3,... NUMNP
		PL(I)	16-30	Load induced at Time PT(I).	For Default values for SIGY, Leave Columns 61-75 Blank.
		DELTA(I)	31-45	Joint Opening at Time PT(I).	
		TEMP(I)	46-60	Temp. at Time PT(I).	
		SIGY(I)	61-75	Fracture Strength of the Overlay Material at Time PT(I).	

APPENDIX B

Theoretical analysis of small scale beams described in Mechanistic Methodology for Airport Pavement Design with Engineering Fabrics, Volume I: Theoretical and Experimental Bases.

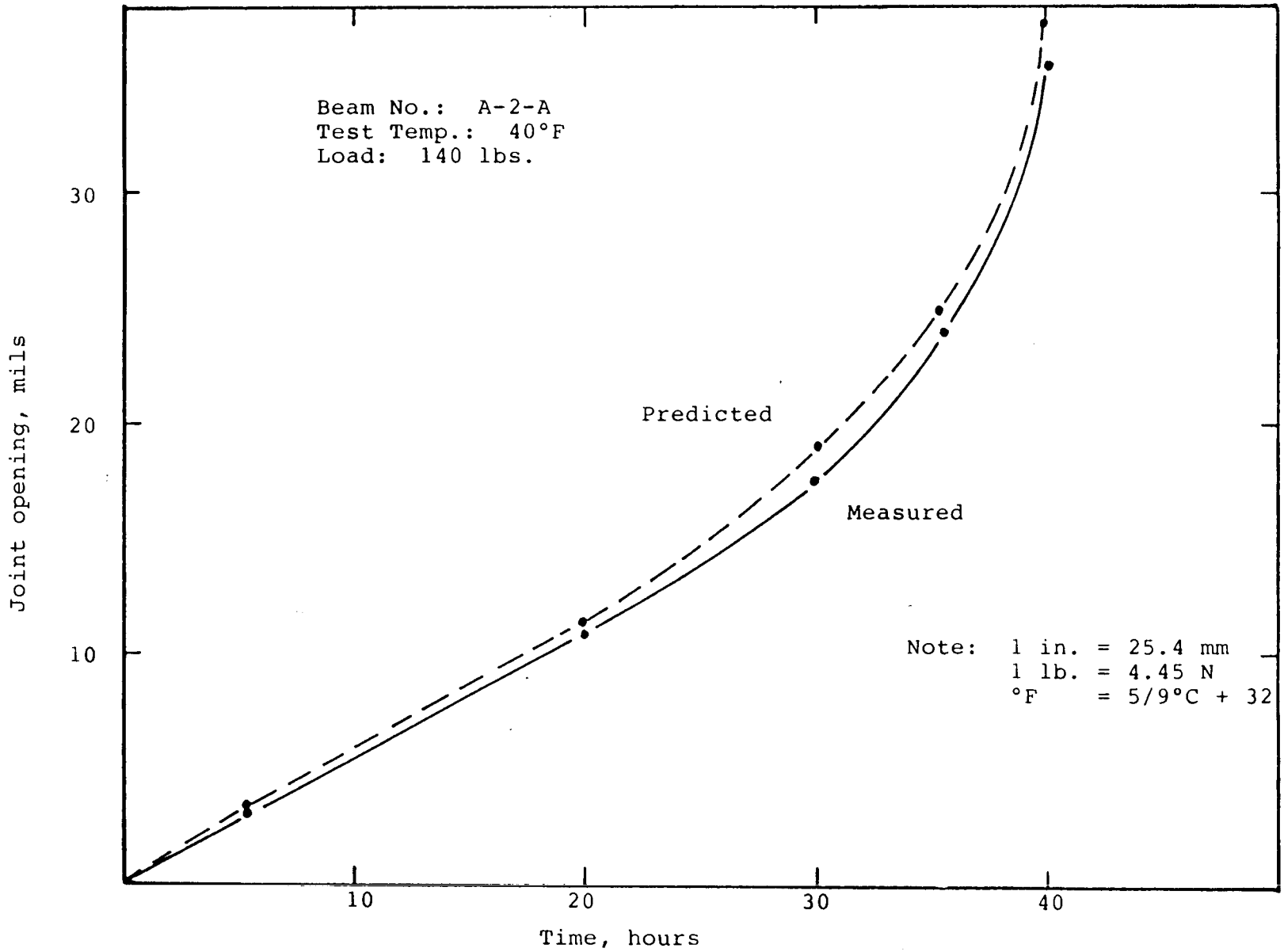

Figure 16. Joint opening vs time for small-scale beams.

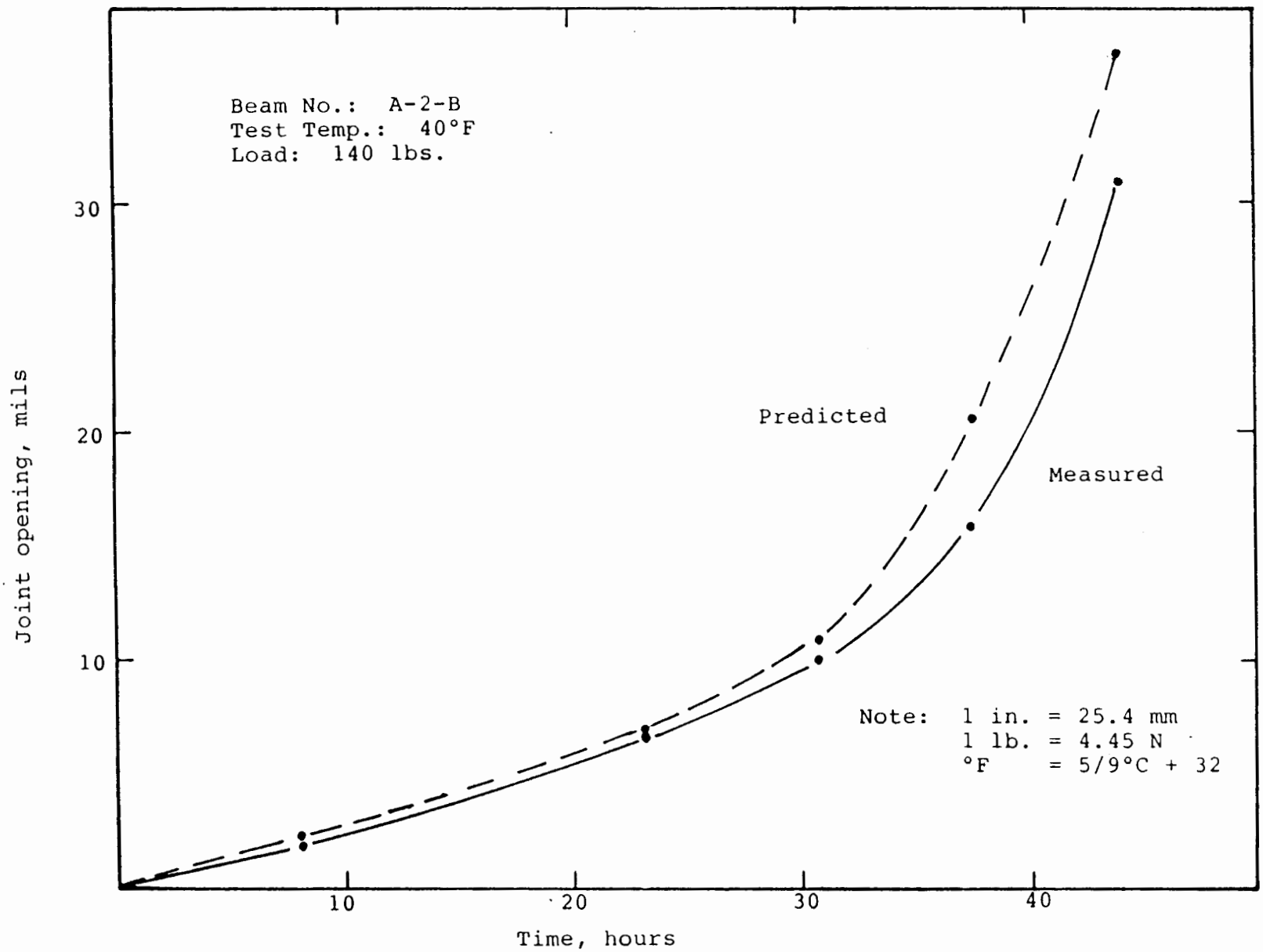

Figure 17. Joint opening vs time for small-scale beams.

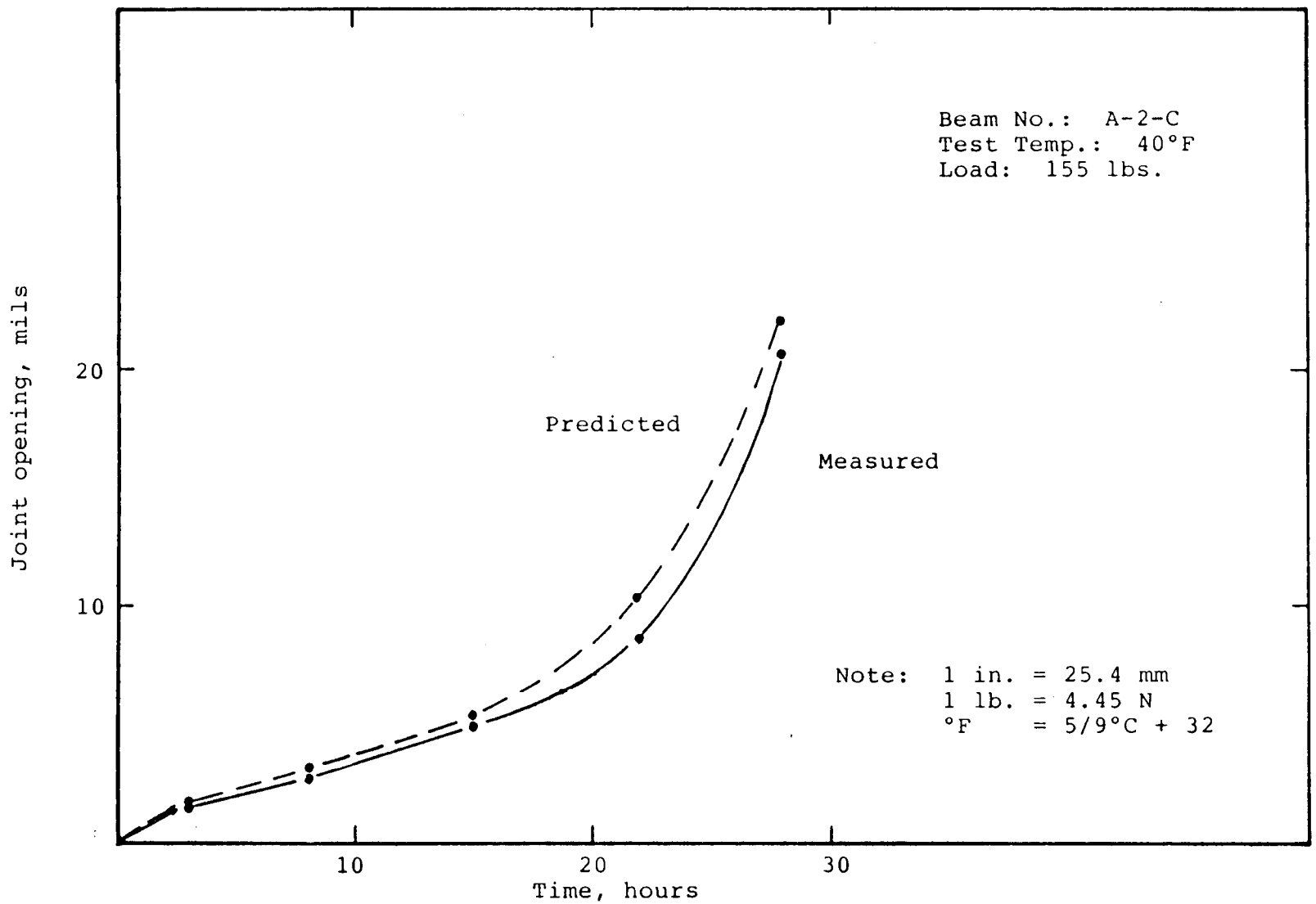

Figure 18. Joint opening vs time for small-scale beams.

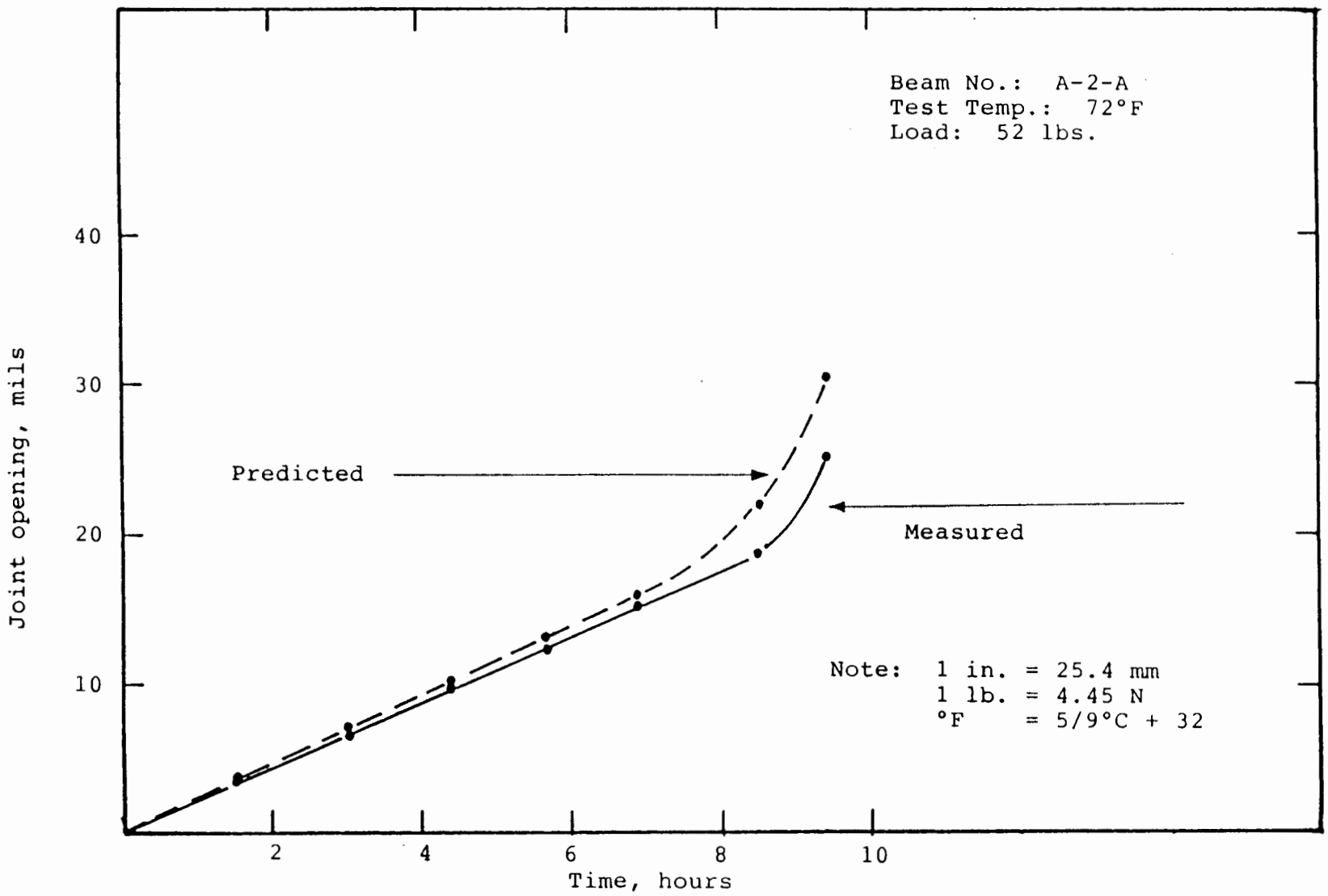

Figure 19. Joint opening vs time for small-scale beams.

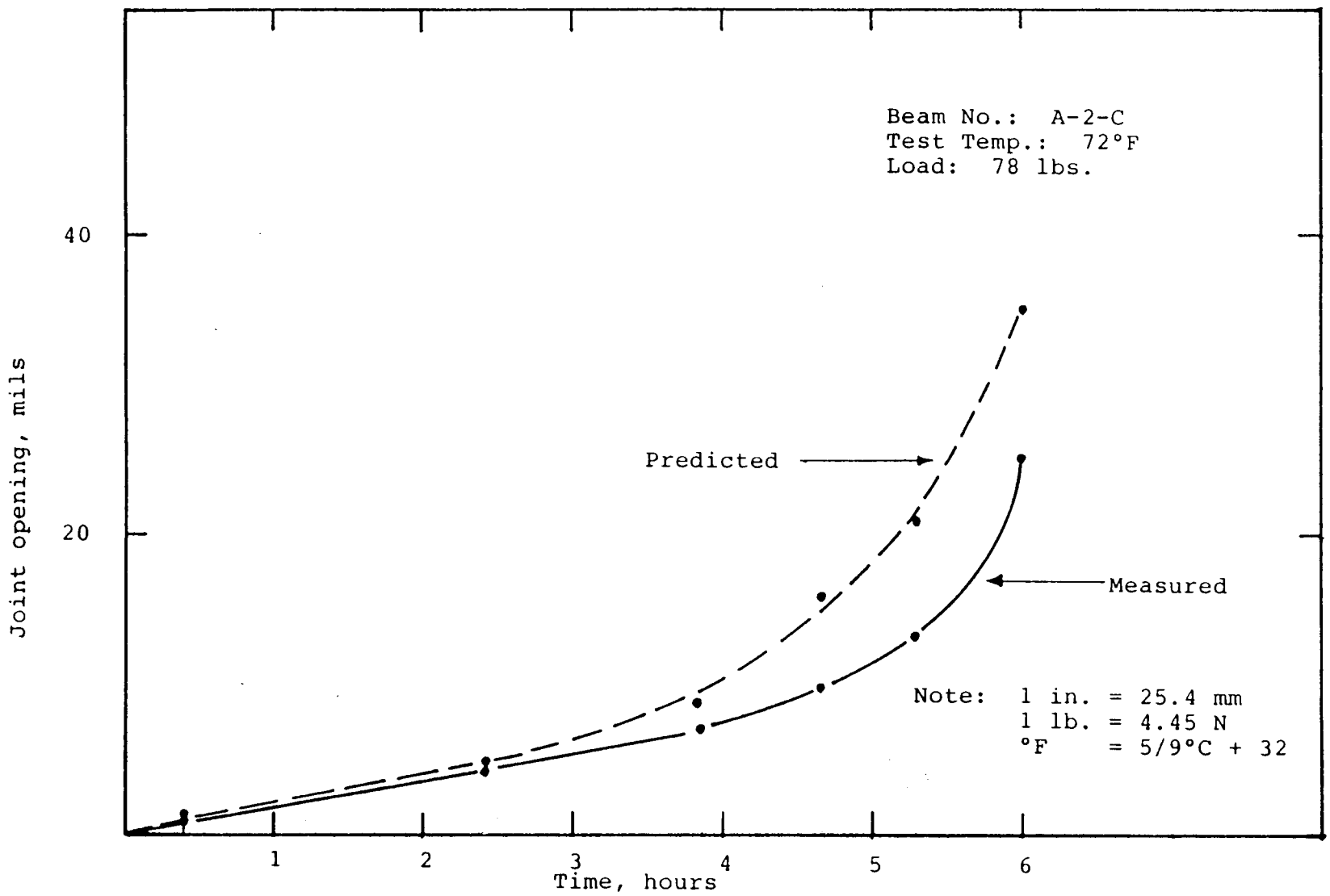

Figure 20. Joint opening vs time for small-scale beams.

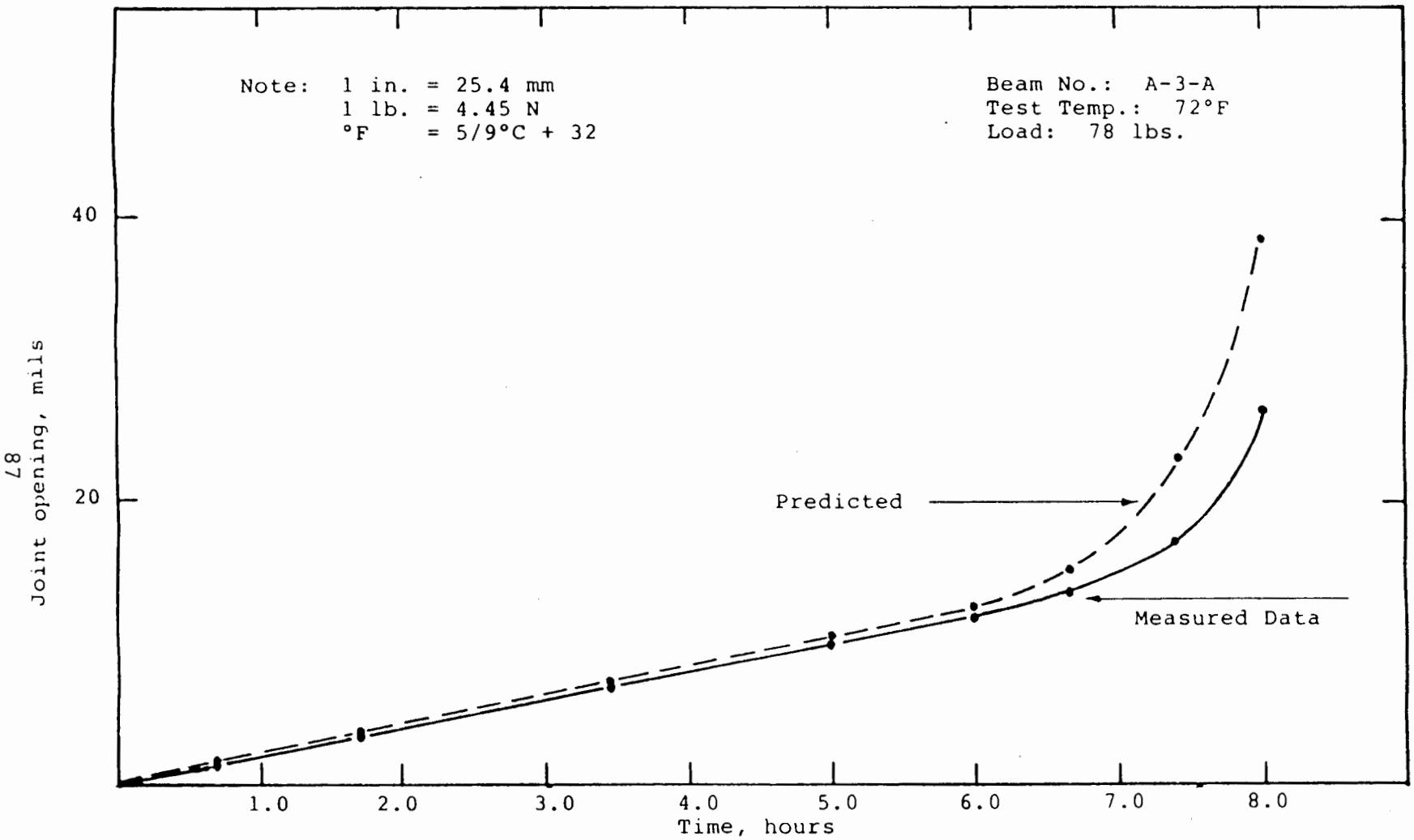

Figure 21. Joint opening vs time for small-scale beams.